

1 **A comprehensive sulfur and oxygen isotope study of sulfur cycling in a shallow, hyper-**  
2 **euxinic meromictic lake**

3  
4  
5  
6  
7  
8  
9  
10  
11  
12  
13  
14  
15  
16  
17  
18  
19  
20  
21  
22

William P. Gilhooly III<sup>a,b,\*</sup>, Christopher T. Reinhard<sup>a,c</sup>, Timothy W. Lyons<sup>a</sup>

<sup>a</sup>Department of Earth Sciences, University of California, 900 University Avenue, Riverside, CA 92521, USA

<sup>b</sup>Department of Earth Sciences, Indiana University-Purdue University Indianapolis, SL118, 723 W. Michigan Street, Indianapolis, IN 46202, USA

<sup>c</sup>School of Earth & Atmospheric Sciences, Georgia Institute of Technology, 311 Ferst Drive, Atlanta, GA 30332, USA

\*Corresponding author. Current address: Department of Earth Sciences, Indiana University-Purdue University Indianapolis, SL118, 723 W. Michigan Street, Indianapolis, IN 46202, USA.  
E-mail address: [wgilhool@iupui.edu](mailto:wgilhool@iupui.edu) (W. Gilhooly).

---

This is the author's manuscript of the article published in final edited form as:

Gilhooly III, W. P., Reinhard, C. T., & Lyons, T. W. (n.d.). A comprehensive sulfur and oxygen isotope study of sulfur cycling in a shallow, hyper-euxinic meromictic lake. *Geochimica et Cosmochimica Acta*.  
<http://doi.org/10.1016/j.gca.2016.05.044>

23 **Abstract**

24 Mahoney Lake is a permanently anoxic and sulfidic (euxinic) lake that has a dense plate of  
25 purple sulfur bacteria positioned at mid-water depth (~ 7 m) where free sulfide intercepts the  
26 photic zone. We analyzed the isotopic composition of sulfate ( $\delta^{34}\text{S}_{\text{SO}_4}$  and  $\delta^{18}\text{O}_{\text{SO}_4}$ ), sulfide  
27 ( $\delta^{34}\text{S}_{\text{H}_2\text{S}}$ ), and the water ( $\delta^{18}\text{O}_{\text{H}_2\text{O}}$ ) to track the potentially coupled processes of dissimilatory  
28 sulfate reduction and phototrophic sulfide oxidation within an aquatic environment with  
29 extremely high sulfide concentrations (>30 mM). Large isotopic offsets observed between sulfate  
30 and sulfide within the monimolimnion ( $\delta^{34}\text{S}_{\text{SO}_4\text{-H}_2\text{S}} = 51\text{‰}$ ) and within pore waters along the oxic  
31 margin ( $\delta^{34}\text{S}_{\text{SO}_4\text{-H}_2\text{S}} > 50\text{‰}$ ) are consistent with sulfate reduction in both the sediments and the  
32 anoxic water column. Given the high sulfide concentrations of the lake, sulfur disproportionation  
33 is likely inoperable or limited to a very narrow zone in the chemocline, and therefore the large  
34 instantaneous fractionations are best explained by the microbial process of sulfate reduction.  
35 Pyrite extracted from the sediments reflects the isotopic composition of water column sulfide,  
36 suggesting that pyrite buried in the euxinic depocenter of the lake formed in the water column.  
37 The offset between sulfate and dissolved sulfide decreases at the chemocline ( $\delta^{34}\text{S}_{\text{SO}_4\text{-H}_2\text{S}} =$   
38  $37\text{‰}$ ), a trend possibly explained by elevated sulfate reduction rates and inconsistent with  
39 appreciable disproportionation within this interval. Water column sulfate exhibits a linear  
40 response in  $\delta^{18}\text{O}_{\text{SO}_4}\text{-}\delta^{34}\text{S}_{\text{SO}_4}$  and the slope of this relationship suggests relatively high sulfate  
41 reduction rates that appear to respond to seasonal changes in the productivity of purple sulfur  
42 bacteria. Although photosynthetic activity within the microbial plate influences the  $\delta^{18}\text{O}_{\text{SO}_4}\text{-}\delta^{34}\text{S}$   
43 relationship, the biosignature for photosynthetic sulfur bacteria is restricted to the oxic/anoxic  
44 transition zone and is apparently minor relative to the more prevalent process of sulfate reduction  
45 operative throughout the light-deprived deeper anoxic water column and sediment pore waters.

46

47 **1. Introduction**

48 Sulfur isotope compilations of sedimentary pyrite and sulfates (gypsum, barite, carbonate-  
49 associated sulfate) have provided proxy evidence for the increase in atmospheric oxygen from  
50 the Archean to the present. Three distinct stages have been recognized in the sulfur isotope  
51 record based on mass conservative ( $^{34}\text{S}/^{32}\text{S}$ ) and mass-independent ( $^{33}\text{S}/^{32}\text{S}$ ) fractionation effects.  
52 Small  $\delta^{34}\text{S}$  fractionations (Canfield, 1998), associated with low oceanic sulfate levels ( $< 2.5 \mu\text{M}$ )  
53 in the Archean (Habicht et al., 2002; Crowe et al., 2014), are congruent with  $\Delta^{33}\text{S}$  photochemical  
54 isotope effects preserved under low atmospheric oxygen levels (Farquhar et al., 2000). This  
55 stage ends with the Great Oxidation Event marked by an increase in  $\delta^{34}\text{S}$  fractionations  
56 coincident with the loss of mass-independent signatures  $\sim 2.3$ - $2.4$  billion years ago (Bekker et al.,  
57 2004), indicating that oxygen accumulated to significant concentrations in the atmosphere. The  
58 third state, characterized by frequently large fractionations perhaps linked to a strongly oxidative  
59 sulfur cycling and analogous to isotopic patterns seen today ( $\Delta^{34}\text{S}_{\text{sulfate-sulfide}} > 50\text{‰}$ ), commenced  
60 during the Neoproterozoic (1050 to 640 million years ago) (Canfield & Teske, 1996; Canfield,  
61 2001).

62  
63 The isotopic offset ( $\Delta^{34}\text{S}_{\text{sulfate-sulfide}} = \delta^{34}\text{S}_{\text{sulfate}} - \delta^{34}\text{S}_{\text{sulfide}}$ ) imparted during dissimilatory sulfate  
64 reduction can be large in magnitude, with  $\Delta^{34}\text{S}_{\text{sulfate-sulfide}}$  exceeding  $60\text{‰}$  (Canfield et al., 2010;  
65 Sim et al., 2011), or muted ( $\sim 0\text{‰}$ ) at low sulfate concentrations (Harrison & Thode, 1958;  
66 Habicht et al., 2002). Similar offsets are produced by the oxidative sulfur cycle, ranging from the  
67 potentially large isotope effects ( $\sim 20\text{‰}$ ) that can occur during sulfur disproportionation  
68 (Canfield & Thamdrup, 1994; Habicht et al., 1998; Böttcher et al., 2001) to small isotope effects  
69 ( $\pm 5\text{‰}$ ) produced during chemolithotrophic sulfide oxidation (Fry et al., 1986) and anoxygenic

70 photosynthesis (Fry et al., 1984; Fry, 1986; Zerkle et al., 2009; Brabec et al., 2012). An  
71 otherwise robust biosignature for sulfate reduction in modern sediments thus becomes non-  
72 diagnostic under sulfate-limited conditions as postulated for the Archean ocean or periods of  
73 rapid expansion of the oceanic sulfate pool such as the Neoproterozoic, when many reactions  
74 within the biologically mediated sulfur cycle may be operative. For example, the various  
75 explanations for an increase in the magnitude of sulfur isotope fractionations during the  
76 Neoproterozoic include an increased prominence of nonphotosynthetic oxidative sulfur  
77 metabolisms and associated disproportionation of the resulting intermediate sulfur species  
78 (Canfield & Teske, 1996; Johnston et al., 2005; Fike et al., 2006), reoxidation effects mediated  
79 by the onset of bioturbation (Canfield & Farquhar, 2009), and possibly reservoir effects linked  
80 with rising and falling sulfate concentrations within an evolving oceanic sulfur pool (Hurtgen et  
81 al., 2005).

82  
83 The isotopic composition of oxygen bound in sulfate ( $\delta^{18}\text{O}_{\text{SO}_4}$ ) may provide an additional vector  
84 to better interpret the microbial processes responsible for sulfate synthesis and cycling over  
85 geologic timescales. Provided the associated isotope effects are constrained,  $\delta^{18}\text{O}_{\text{SO}_4}$  can be a  
86 powerful tool for tracing the ultimate source of sulfate to the ocean, given that the oxygen  
87 incorporated into the sulfate during sulfide oxidation can derive from either ambient water ( $\text{H}_2\text{O}$ )  
88 or the atmosphere ( $\text{O}_2$ ). On a global basis, gypsum dissolution and oxidative pyrite weathering  
89 (the inputs) balance the outputs via evaporite precipitation and sulfate reduction with  
90 concomitant pyrite burial (Holser et al., 1979; Claypool et al., 1980). Tracking the sulfate-  
91 oxygen budget through these isotopically distinct reservoirs is complicated by oxygen isotope  
92 exchange at low pH (Hoering & Kennedy, 1957; Lloyd, 1968; Chiba & Sakai, 1985), post-

93 diagenetic alteration (Turchyn et al., 2009), and numerous other processes that overprint the  
94 oxygen isotope composition of sulfate (Bottrell & Newton, 2006; Turchyn & Schrag, 2006).

95  
96 Sulfur isotopes are relatively insensitive to inorganic sulfide oxidation effects, but sulfate formed  
97 from sulfide oxidation will carry different proportions of oxygen derived from water ( $\delta^{18}\text{O} \leq$   
98  $0\text{‰}$ ) and/or atmospheric oxygen ( $\delta^{18}\text{O} = 23.5\text{‰}$ ) depending on the oxidation pathway (Taylor &  
99 Wheeler, 1984; van Everdingen & Krouse, 1985; Balci et al., 2007; Calmels et al., 2007; Balci et  
100 al., 2012). The oxidation of sulfide coupled to iron reduction derives oxygen entirely from water  
101 and results in  $\delta^{18}\text{O}_{\text{SO}_4}$  values lower than those produced by oxidation with molecular oxygen  
102 (Calmels et al., 2007). Hydrothermal sulfur inputs ( $\sim 0\text{‰}$ ) may be difficult to differentiate from  
103 biological cycling within a low sulfate reservoir; however,  $\delta^{18}\text{O}_{\text{SO}_4}$  produced by photosynthetic  
104 bacteria may reflect the isotopic composition of the parent water (Brabec et al., 2012).

105  
106 Environmental conditions in the Paleo- and Mesoproterozoic, when atmospheric oxygen  
107 concentrations were still relatively low, and large portions of the oceans were anoxic and sulfidic  
108 (euxinic), were conducive to widespread carbon fixation by anoxygenic photosynthesis  
109 (Johnston et al., 2009). Phototrophic sulfur bacteria oxidize sulfide and fix carbon dioxide in the  
110 presence of sunlight without producing oxygen. Sulfide is oxidized to intracellular elemental  
111 sulfur, and the internal sulfur stores are ultimately oxidized to sulfate when sulfide becomes  
112 limiting ( $< 1 \text{ mM}$ ) (Overmann & Pfennig, 1992). In the geologic record, this ecological niche is  
113 termed “photic zone euxinia,” and organic biomarkers of sulfide-oxidizing phototrophs can  
114 provide proxy evidence for free sulfide at shallow depths in the water column (Brocks et al.,  
115 2005; Brocks & Schaeffer, 2008) provided the organisms were pelagic (Meyer et al., 2011).

116 Biological oxidation of sulfide by anoxygenic photosynthesis may have contributed to the  
117 formation of sulfate in the Proterozoic water column (Johnston et al., 2009). With limited  
118 organic biomarker and geochemical evidence for widespread primary production by anoxygenic  
119 sulfur bacteria (Lyons et al., 2004), and the potential for metabolic overlap with cyanobacteria  
120 capable of sulfide oxidation but without a distinctive biomarker signature for this process  
121 (Johnston et al., 2009), additional proxies are needed to fingerprint the paleoecological and  
122 biogeochemical signals associated with euxinia in the photic zone. Paired  $\delta^{34}\text{S}$  and  $\delta^{18}\text{O}$  data  
123 from ancient sulfates (gypsum, barite, or carbonate-associated-sulfate) may offer an additional  
124 constraint on the history and ecological distribution of photosynthetic S-oxidation. Sulfate-  
125 oxygen can fractionate during sulfate reduction, but the extent of isotopic enrichment is  
126 controlled either by kinetic isotope effects imparted during intracellular enzymatic steps or  
127 equilibrium oxygen exchange with ambient water (Brunner et al., 2005; Brunner et al., 2012;  
128 Antler et al., 2013). An improved understanding of these processes can be gained from modern  
129 natural environments.

130  
131 The primary objective of this study was to track microbial sulfur oxidation and reduction in  
132 density stratified Mahoney Lake as a modern analog for biotic pathways that may have generated  
133 oxidants in Earth's early ocean. Free dissolved sulfide ( $[\text{H}_2\text{S}] = 30 \text{ mM}$ ) in the photic zone of the  
134 water column supports a perennial plate of purple sulfur bacteria (Northcote & Halsey, 1969;  
135 Northcote & Hall, 1983; Overmann et al., 1991; Overmann et al., 1996). The purple sulfur  
136 bacterium is a member of *Chromatiaceae* and is designated as strain ML1 (Hamilton et al.,  
137 2014). Although found at mid-water depth of the lake, ML1 is most closely related to a marine  
138 benthic purple sulfur bacteria *Thiohalocapsa* (Hamilton et al., 2014). Such observations have

139 significance when relating biomarker distribution to microbial ecology and inferred  
140 environmental conditions (Meyer et al., 2011). The euxinic conditions are broadly consistent  
141 with chemical properties for many Proterozoic ocean models (Reinhard et al., 2013). However,  
142 the lake also has high sulfate concentrations ( $[\text{SO}_4] > 300 \text{ mM}$ ) that are inconsistent with early  
143 analogs and indeed are more than ten times the concentration in the modern ocean. At the same  
144 time, the large reservoir helps maximize the isotopic offset for sulfate reduction ( $\Delta^{34}\text{S}_{\text{sulfate-sulfide}}$   
145  $> 50\text{‰}$ ). In other words, the isotopic offsets are controlled by biological processing rather than by  
146 the size of the sulfate pool. The biosignature for dissimilatory sulfate reduction in Mahoney Lake  
147 is thus distinct from the small offsets produced under sulfate-limited conditions that would  
148 otherwise overlap with sulfur isotope fractionations produced by sulfide oxidizing phototrophic  
149 bacteria. As such, Mahoney Lake provides a novel natural laboratory for studying sulfur cycling.

150 We present paired sulfur and oxygen isotope compositions of dissolved sulfate ( $\delta^{34}\text{S}_{\text{SO}_4}$  and  
151  $\delta^{18}\text{O}_{\text{SO}_4}$ ) relative to the sulfur isotope properties of product sulfides (either dissolved or  
152 sedimentary) to explore isotope effects associated with sulfate reduction and anaerobic sulfide  
153 oxidation (and thus biologically mediated sulfate generation) by anoxygenic photosynthetic  
154 bacteria.

155

## 156 **2. Materials and Methods**

### 157 *Site description*

158 Mahoney Lake (49°17'N; 119°35'W; elevation 47.15 m) is a permanently stratified (meromictic)  
159 lake in the Okanagan Valley, British Columbia (Figure 1). Within the same catchment, Green  
160 Lake (49°18'N, 119°34'W, 490.7 m) fully mixes during fall and spring overturn (dimictic). Both  
161 are shallow (~15 m), saline, terminal lakes. The Okanagan Valley is an arid region within the

162 southern interior of a province that receives an average of 265 mm of total annual precipitation  
163 (rain and snow). Mean monthly temperatures range from -14.3°C to 23.5°C  
164 (www.climate.weatheroffice.gc.ca; station 1126150; precipitation and temperature records 1941  
165 to 2010).

166  
167 The lake drainage area is located within an extensional basin known as the White Lake Basin  
168 (Figure 1). The regional geology is dominated by a complex series of normal faults, fractured  
169 bedding planes, and jointed volcanic formations that promote groundwater circulation (Lewis,  
170 1984; Michel et al., 2002). Both lakes straddle a north-south trending fault line that bisects the  
171 drainage basin (Northcote & Hall, 1983). The bedrock geology to the east of the fault is  
172 comprised of cherts, greenstones, schists, and granitic intrusions (Northcote & Hall, 1983;  
173 Church, 2002) (Figure 1). The western extent of the catchment contains ultramafic volcanic  
174 rocks and lavas (Northcote & Hall, 1983; Church, 2002). Salts (Na-Ca-Mg-SO<sub>4</sub>) derived from  
175 the weathering of metavolcanic rocks from the Marron Formation (Eocene) in the surrounding  
176 watershed contribute to the high conductivity and total dissolved solid load of Mahoney Lake  
177 (Northcote & Hall, 1983).

178  
179 Mahoney Lake (136.2x10<sup>4</sup> m<sup>3</sup>, 19.8 ha, 6.9 m) and Green Lake (113.6x10<sup>4</sup> m<sup>3</sup>, 12.6 ha, 9.0 m)  
180 have similar volumes, surface areas, and mean depths (Northcote & Hall, 1983). Although the  
181 dimensions of the lakes are comparable, water column redox conditions are strikingly different.  
182 The Mahoney Lake monimolimnion persistently contains dissolved sulfide, whereas bottom  
183 waters in Green Lake are perennially saturated with oxygen. The similar physical features  
184 suggest other factors are responsible for meromixis in Mahoney Lake. Northcote and Hall (1983)



185 proposed that the hills surrounding Mahoney shelter the lake from prevailing winds and thus  
186 wind-blown mixing. In contrast, Green Lake is exposed to strong northeasterly winds that  
187 routinely mix the water column (Ward et al., 1989; Ward et al., 1990).

188  
189 Sediments and pore waters were extracted from Cores 2 and 3 collected within the euxinic water  
190 mass from the deepest portion of Mahoney Lake in September 2006; Core 9 was collected at the  
191 same time along the oxic margin above the chemocline (Figure 1). Water column samples were  
192 also collected from Green Lake as a reference for oxic conditions in a saline lake. Water column  
193 samples were collected from Mahoney Lake in September 2006 and July 2008. During the later  
194 trip, water was also sampled from a shallow pond (< 1 m) in the hills to the west ('ML pond')  
195 and from Sleeping Lake to the east (Figure 1).

196

#### 197 *Water column sampling*

198 Photosynthetically available radiation was measured with a spherical light sensor (LI-193, LI-  
199 COR Environmental, Lincoln, NE, USA). Light attenuation above and below the microbial plate  
200 was determined according to Beer-Bouguer's Law:

201

$$202 \quad I_z = I_0 e^{-kz}, \quad (1)$$

203

204 where radiation incident at depth ( $I_z$ ) is proportional to the light intensity from the surface ( $I_0$ )  
205 and the extinction coefficient ( $k$ ) at a given depth ( $z$ ). Turbidity was measured as an indication of  
206 water clarity and microbial biomass (2020c Turbidimeter, LaMotte Company, Chestertown, MD,  
207 USA). Water column pH, temperature, specific conductivity, and dissolved oxygen profiles were

208 measured *in situ* with a handheld meter and probe (Quanta, Hydrolab, Loveland, CO, USA).  
209 Water column samples were collected with a battery-powered pump at depth intervals of 10 to  
210 100 cm. High-resolution samples were also collected in the water column with a syringe sampler  
211 that allowed sampling at fixed intervals (10 cm) with minimal disturbance of the chemocline.  
212 The dissolved oxygen meter was attached to the base of the syringe sampler, and the position of  
213 the syringe ports relative to the location of the oxic-anoxic interface was determined from the  
214 oxygen concentrations measured *in situ* and the known distance between the syringes and the  
215 probe. Samples from the water column collected for sulfide analysis were preserved with 3%  
216 (wt./volume) zinc acetate solution for concentration determinations or precipitated with cadmium  
217 acetate for sulfur isotope analysis. A subset of samples from the water column was taken for  
218 elemental sulfur were filtered onto 0.2  $\mu\text{m}$  polyestersulfone filters (Millipore) under nitrogen  
219 atmosphere and stored frozen at  $-20^{\circ}\text{C}$ .

220

### 221 *Sediments and pore waters*

222 Lake sediments were collected with a modified gravity-piston corer (Fisher et al., 1992).  
223 Sediment cores were capped, sealed, and taken to the field laboratory for processing within hours  
224 of collection. Sediments were sectioned and extruded in a nitrogen-filled glovebag. Surfaces of  
225 the whole-round mud samples in contact with the core liner were scrapped to remove potential  
226 lake water contamination and to minimize the effects of smearing. Pore waters were extracted by  
227 centrifugation and filtered through 0.2  $\mu\text{m}$  syringe filters. Pore water splits were preserved for  
228 sulfide concentrations with 3% (wt./volume) zinc acetate solution or precipitated with cadmium  
229 acetate for sulfur isotope analysis. Sediment samples were then purged with nitrogen gas, frozen,  
230 and transported to our labs in Riverside for subsequent analyses.

231

232 *Analytical*

233 Sedimentary sulfides were extracted from wet, freshly thawed sediment by sequential  
234 extractions. Water content was determined by weighing separate sediment splits before and after  
235 drying and corrected for mass addition from salts that precipitated during sample drying in order  
236 to present the data as wt.% on a dry sediment basis. Acid volatile sulfides (AVS; FeS) were  
237 extracted with a room temperature solution of 6N HCl and 15% (wt./volume) stannous chloride  
238 (Chanton & Martens, 1985; Cornwell & Morse, 1987). The extractant was subsequently  
239 separated from the sediment by filtration onto a glass fiber filter, and chromium reducible sulfide  
240 (CRS; pyrite and elemental sulfur) was then liberated from the filtered residue by reaction with a  
241 solution of boiling 1M chromous chloride and concentrated HCl (Canfield et al., 1986).  
242 Chromium reducible sulfide (dominantly pyrite in this case) was also extracted from a  
243 greenstone rock sample collected within the catchment. Hydrogen sulfide evolved from these  
244 distillations was trapped in 3% zinc acetate solution for concentration measurements by  
245 iodometric titration or precipitated as Ag<sub>2</sub>S in a solution of 3% silver nitrate and 10% ammonium  
246 hydroxide for sulfur isotope analysis (wt./volume).

247

248 The degree of sulfurization (DOS) (Boesen & Postma, 1988; Raiswell et al., 1994) was  
249 determined according to the relationship:

250

$$251 \text{DOS} = \frac{\text{Fe}_{\text{AVS}} + \text{Fe}_{\text{py}}}{\text{Fe}_{\text{AVS}} + \text{Fe}_{\text{py}} + \text{Fe}_{\text{HCl}}} \quad (2)$$

252 where Fe<sub>AVS</sub> and Fe<sub>py</sub> are the concentrations of AVS-iron and pyrite-iron calculated from  
253 extracted concentrations of AVS-sulfur and pyrite-sulfur and assuming the respective

254 stoichiometries of FeS and FeS<sub>2</sub>. Reactive iron, Fe<sub>HCl</sub>, was extracted from dried sediment with  
255 boiling 12N HCl (Berner, 1970; Raiswell et al., 1988), and extractable iron concentrations were  
256 measured by the Ferrozine colorimetric method (Stookey, 1970). High DOS values, approaching  
257 unity in extreme cases, indicate formation and accumulation of sedimentary iron-sulfide minerals  
258 under euxinic (iron-limited) conditions.

259  
260 Dissolved sulfide in the water column and pore waters was preserved in the field with zinc  
261 acetate or cadmium acetate followed by centrifugation, and aliquots of the supernatant were  
262 isolated for determining chloride and sulfate concentrations. Dissolved sulfide concentrations  
263 were determined colorimetrically (Cline, 1969). Sulfate concentrations were measured  
264 gravimetrically or as dissolved S by ICP-MS with Xe as the collision cell gas (Agilent 7400  
265 Quadrupole ICP-MS). Sulfate concentrations determined by either method agreed within ±5%.  
266 Chloride concentrations were measured by titration (DP-957M Digital Chloridometer, Haake  
267 Buchler Instruments Inc., Saddlebrook, NJ, USA). Supernatant splits were also taken for sulfur  
268 and oxygen isotope analysis of sulfate. The addition of zinc acetate to water column and pore  
269 water samples caused the dissolved sulfide to precipitate immediately and thus precluded  
270 secondary sulfate contributions from sulfide oxidation. Sulfate was precipitated as BaSO<sub>4</sub> by  
271 addition of saturated BaCl<sub>2</sub> solution (250 g/L) followed by brief acidification (4N HCl) to  
272 remove carbonates, rinsing to neutral pH, and drying. Elemental sulfur was extracted from  
273 filters collected from the water column onto copper turnings using hexane and sonication, which  
274 was subsequently liberated by chromium reduction (Canfield et al., 1986) and trapped in silver  
275 nitrate. Sulfides fixed as CdS in the field were rinsed with deionized water and reprecipitated as  
276 Ag<sub>2</sub>S by addition of 3% silver nitrate and 10% ammonium hydroxide (wt./volume). Precipitates

277 of sulfate ( $\text{BaSO}_4$ ) and sulfide ( $\text{Ag}_2\text{S}$ ) derived from sediment extracts or dissolved species were  
278 dried and homogenized with agate mortar and pestle prior to isotopic analysis.

279

280 Isotope compositions were expressed according to the equation:

281

$$282 \quad \delta^x\text{E} = \left[ \left( R_{\text{sample}} / R_{\text{standard}} \right) - 1 \right] \times 1000 \quad (3)$$

283

284 where  $^x\text{E}$  is the given isotope ( $^2\text{H}$ ,  $^{18}\text{O}$ , or  $^{34}\text{S}$ ), and  $R$  is the  $^2\text{H}/^1\text{H}$ ,  $^{18}\text{O}/^{16}\text{O}$ , or  $^{34}\text{S}/^{32}\text{S}$  ratio  
285 relative to the respective international standards for H and O (V-SMOW), and S (V-CDT).

286 Water column samples were distilled prior to hydrogen and oxygen isotope analysis (West et al.,

287 2006) and analyzed at the Purdue Stable Isotope Facility, Purdue University, using a Thermo-

288 Chemical Elemental Analyzer coupled with a stable isotope ratio mass spectrometer (TCEA-

289 IRMS; Delta V; ThermoElectron, Bremen, Germany). Analytical precision was better than

290  $\pm 0.1\text{‰}$  for  $\delta\text{D}_{\text{H}_2\text{O}}$  and  $\pm 0.2\text{‰}$  for  $\delta^{18}\text{O}_{\text{H}_2\text{O}}$ . Sulfur isotope ratios of the sulfide phases and sulfur

291 and oxygen isotopes of sulfate were analyzed on a Delta V Plus IRMS (ThermoElectron,

292 Bremen, Germany) at the Department of Earth Sciences, University of California, Riverside.

293 Samples precipitated as either  $\text{Ag}_2\text{S}$  or  $\text{BaSO}_4$  were weighed into tin capsules with a ten-fold

294 excess of  $\text{V}_2\text{O}_5$  for a final sample mass of  $\sim 50 \mu\text{g-S}$  and combusted on an ECS elemental

295 analyzer (Costech Analytical, USA) coupled under continuous flow to the IRMS.  $\delta^{34}\text{S}_{\text{BaSO}_4}$

296 values were normalized to international standards NBS-127 (21.1‰), IAEA SO-5 (0.49‰), and

297 IAEA SO-6 (-34.05‰). Values for  $\delta^{34}\text{S}_{\text{Ag}_2\text{S}}$  were normalized to IAEA standards S1 (-0.3‰), S2

298 (22.65‰), and S3 (-32.5‰).  $\delta^{18}\text{O}_{\text{SO}_4}$  values were determined by TCEA-IRMS and calibrated

299 against NBS-127 (8.7‰), IAEA SO-5 (12.0‰), and IAEA SO-6 (-11.0‰). Reproducibility of

300 standard reference materials and sample replicates were  $\pm 0.2\%$  for  $\delta^{34}\text{S}$  and  $\pm 0.4\%$  for  $\delta^{18}\text{O}_{\text{SO}_4}$ .

301

302 ***Sulfate reduction models of  $\delta^{34}\text{S}_{\text{SO}_4}$  and  $\delta^{18}\text{O}_{\text{SO}_4}$***

303 Linear and non-linear regressions of  $\delta^{18}\text{O}_{\text{SO}_4}$  and  $\delta^{34}\text{S}_{\text{SO}_4}$  (Böttcher et al., 1998; Brunner et al.,  
304 2005; Brunner et al., 2012; Antler et al., 2013) can provide insight into the relative rates of  
305 sulfate reduction and the extent of back reaction that occurs during intracellular cycling of sulfur  
306 intermediates. We use models, developed by Antler et al., (2013), that couple the sulfur and  
307 oxygen isotope (kinetic and equilibrium) fractionations that occur during sulfate reduction to  
308 provide a framework for interpreting the isotopic variation observed in Mahoney Lake. Antler et  
309 al. (2013) defined two trends that describe linear (Trend A) and curvilinear (Trend B) responses  
310 in  $\delta^{18}\text{O}$ - $\delta^{34}\text{S}$  isotope space (Figure 7A). We briefly describe their models here, but full details  
311 and explanations of their assumptions are provided in Antler et al. (2013).

312

313 The models are sensitive to the ratio of the forward and backward fluxes ( $X = b/f$ ) of sulfur  
314 within the cell and the associated kinetic isotope fractions ( $\epsilon$ ) that occur during three steps in the  
315 sulfate reduction network. The steps include sulfate uptake into the cell ( $X_1$ ;  $\epsilon^{34}\text{S} = -3\%$ ;  $\epsilon^{18}\text{O} = -$   
316  $0.75\%$ ), the reduction of adenosine 5'-phosphosulfate (APS) to sulfite ( $X_2$ ;  $\epsilon^{34}\text{S} = 25\%$ ;  $\epsilon^{18}\text{O} =$   
317  $6.25\%$ ), and the reduction of sulfite to sulfide ( $X_3$ ;  $\epsilon^{34}\text{S} = 25\%$ ;  $\epsilon^{18}\text{O} = 6.25\%$ ) (Mizutani &  
318 Rafter, 1969; Rees, 1973; Antler et al., 2013). The  $\delta^{18}\text{O}$ - $\delta^{34}\text{S}$  isotope pattern is linear (Trend A)  
319 when there is no reverse flux of sulfur ( $X_1 \cdot X_3 = 0$ ) according to the equation,

320

$$321 \delta^{18}\text{O}_{\text{SO}_4(l)} = \frac{\epsilon^{18}\text{O}_{\text{total}}}{\epsilon^{34}\text{S}_{\text{total}}} \cdot \left( \delta^{34}\text{S}_{\text{SO}_4(l)} - \delta^{34}\text{S}_{\text{SO}_4(o)} \right) + \delta^{18}\text{O}_{\text{SO}_4(o)}. \quad (4)$$

322

323 The relationship is non-linear (Trend B) when intracellular recycling (back reaction) occurs  
 324 during sulfate reduction ( $0 < X_1 \cdot X_3 < 1$ ) where,

325

$$326 \delta^{18}\text{O}_{\text{SO}_4(\text{l})} = \delta^{18}\text{O}_{\text{SO}_4(\text{A.E.})} - \exp\left(-\theta_0 \cdot \frac{\delta^{34}\text{S}_{\text{SO}_4(\text{l})} - \delta^{34}\text{S}_{\text{SO}_4(\text{w})}}{\varepsilon^{34}\text{S}_{\text{total}}}\right) \cdot (\delta^{18}\text{O}_{\text{SO}_4(\text{A.E.})} - \delta^{18}\text{O}_{\text{SO}_4(\text{w})}). \quad (5)$$

327

328 The residual sulfate ( $\delta^{18}\text{O}_{\text{SO}_4(\text{l})}$ ) produced by the process of microbial sulfate reduction can thus  
 329 be a linear function (Equation 4) of the total fractionation factors for sulfur and oxygen isotopes  
 330 ( $\varepsilon^{34}\text{S}_{\text{total}}$  and  $\varepsilon^{18}\text{O}_{\text{total}}$ ), the sulfur isotope composition of residual sulfate ( $\delta^{34}\text{S}_{\text{SO}_4(\text{l})}$ ), the initial  
 331 isotopic compositions of sulfate ( $\delta^{34}\text{S}_{\text{SO}_4(\text{w})}$  and  $\delta^{18}\text{O}_{\text{SO}_4(\text{w})}$ ). The oxygen isotope composition of  
 332 sulfate at apparent equilibrium ( $\delta^{18}\text{O}_{\text{SO}_4(\text{A.E.})}$ ) and the relationship ( $\theta_0$ ) between oxygen isotope  
 333 exchange and the rate of sulfate reduction [where  $\theta_0 = (X_1 \cdot X_3)/(1 - X_1 \cdot X_3)$ ] become critical  
 334 parameters in non-linear datasets (Equation 5).

335

### 336 3. Results

#### 337 *Isotopic composition ( $\delta^{34}\text{S}_{\text{SO}_4}$ , $\delta^{18}\text{O}_{\text{SO}_4}$ , $\delta^8\text{O}_{\text{H}_2\text{O}}$ ) of surface waters*

338 The  $\delta^{34}\text{S}_{\text{SO}_4}$  (22.1‰) and  $\delta^{18}\text{O}_{\text{SO}_4}$  (16.7‰) values of surface-water sulfate collected from the  
 339 upper meter of the Mahoney Lake water column resembled dissolved sulfate values in the ML  
 340 pond (Figure 1). In contrast, the isotopic composition of sulfate in Green Lake ( $\delta^{34}\text{S}_{\text{SO}_4} = 1.4‰$   
 341 and  $\delta^{18}\text{O}_{\text{SO}_4} = 10.8‰$ ) and Sleeping Lake ( $\delta^{34}\text{S}_{\text{SO}_4} = 1.6‰$  and  $\delta^{18}\text{O}_{\text{SO}_4} = 10.9‰$ ) were relatively  
 342 depleted in  $^{34}\text{S}$  and  $^{18}\text{O}$ . The low  $\delta^{34}\text{S}$  values of Green and Sleeping lakes were consistent with a  
 343 greenstone sample collected to the east of Mahoney Lake ( $\delta^{34}\text{S}_{\text{Greenstone}} = 0.8‰$ ).

344  
345 Surface waters collected from shallow domestic wells and numerous lakes in the area exhibit  
346 high  $\delta^{18}\text{O}$  and  $\delta\text{D}$  driven by intense rates of evaporation within the arid Okanagan Valley (Figure  
347 2 and references cited therein). Vertical profiles exhibit little variation within the mixolimnion  
348 ( $\delta^{18}\text{O}_{\text{H}_2\text{O}} \approx 0.8\text{‰}$ ) and decrease abruptly across the chemocline to lower values ( $\delta^{18}\text{O}_{\text{H}_2\text{O}} \approx$   
349  $-1.5\text{‰}$ ) within the monomolimnion (Figure 2; Table 1). The slope of the local evaporation line  
350 (4.7) is consistent with evaporation trends observed in hydrologically closed northern latitude  
351 lakes (Gibson et al., 2002; Gibson et al., 2005) (Figure 2).

352

### 353 *Water column chemistry*

354 Representative profiles of water column dissolved oxygen, specific conductivity, temperature,  
355 and pH demonstrate the sharp redox contrast between Green Lake and Mahoney Lake (Figure  
356 3A). Green Lake is well mixed to a depth of 9 m and oxygenated throughout the water column.  
357 In contrast, dissolved oxygen in Mahoney Lake is consumed within 7 m water depth. The  
358 specific conductivity of Mahoney surface waters ( $\sim 43 \text{ mS/cm}$ ) is elevated relative to Green Lake  
359 salinities by an order of magnitude. Conductivity increased 1.5-fold within the monomolimnion  
360 of Mahoney. Water temperatures below the chemocline are isothermal ( $\sim 9^\circ\text{C}$ ) and remain highly  
361 stable relative to inter-annual fluctuations in surface water temperatures (Northcote & Halsey,  
362 1969; Northcote & Hall, 1990; Ward et al., 1990).

363

364 Redox conditions in Mahoney Lake in September 2006 were equivalent to observations made in  
365 July 2008 (compare Figure 3A and 3B). The chemocline was positioned at approximately 7 m



366 during both years. The maximum sulfide concentrations in the water column were extremely  
367 high, ranging from 36 mM (2006) to 41 mM (2008).

368  
369 The plate of purple sulfur bacteria was positioned at the pycnocline where sunlight enters sulfidic  
370 water (Figure 3B). Extinction coefficients increased from the mixolimnion ( $k = 0.400$ ) to the  
371 quantitative absorption of sunlight below the plate ( $k = 3.347$ ) such that less than 0.01% of  
372 incident light penetrated below 8 m water depth. Turbidity is highest within the microbial plate  
373 (Figure 3B). Abundant levels of polysulfides and elemental sulfur (Overmann et al., 1996;  
374 Overmann, 1997) likely contribute to the yellow color of the monomolimnion.

375  
376 Respective chloride and sulfate concentrations averaged  $57.7 \pm 1.7$  mM and  $341.8 \pm 20.1$  mM in  
377 the upper 5 m of the mixolimnion (Figure 4) of Mahoney Lake. Chloride concentrations increased  
378 to approximately 70 mM in the monimolimnion; bottom-water sulfate concentrations were ~500  
379 mM. Molar  $\text{SO}_4/\text{Cl}$  ratios also increased within the bottom waters. Vertical profiles collected  
380 during the two field studies were broadly consistent, with the exception of maxima for sulfate  
381 and chloride concentrations positioned above the chemocline at 6.3 to 6.6 m water depth (2006,  
382 Figure 4), respectively, coincident with a localized decrease in dissolved oxygen concentrations.

383

#### 384 *Isotopic composition ( $\delta^{34}\text{S}_{\text{H}_2\text{S}}$ , $\delta^{34}\text{S}_{\text{SO}_4}$ , $\delta^{18}\text{O}_{\text{SO}_4}$ ) of the Mahoney Lake water column*

385 The  $\delta^{34}\text{S}_{\text{SO}_4}$  and  $\delta^{18}\text{O}_{\text{SO}_4}$  values for samples collected in September 2006 and July 2008 were  
386 similar (Table 1). Relative to the surface, dissolved sulfate exhibited rapid enrichments in  $^{34}\text{S}$  and  
387  $^{18}\text{O}$  across the chemocline and remained fairly constant down to the sediment-water interface  
388 (Figure 4).  $\delta^{34}\text{S}_{\text{SO}_4}$  values within the mixolimnion averaged  $22.1 \pm 0.2\text{‰}$  ( $n = 34$ ) and increased

389 to  $27.7 \pm 0.5\text{‰}$  ( $n = 16$ ) within 0.5 m below the chemocline.  $\delta^{18}\text{O}_{\text{SO}_4}$  values averaged  $17.1 \pm$   
390  $0.4\text{‰}$  ( $n = 34$ ) above the chemocline and increased to  $20.0 \pm 0.6\text{‰}$  ( $n = 34$ ) within the  
391 monimolimnion (7.5 m to bottom). The  $\sim 5.6\text{‰}$  increase in  $\delta^{34}\text{S}_{\text{SO}_4}$  and  $\sim 2.9\text{‰}$  increase in  
392  $\delta^{18}\text{O}_{\text{SO}_4}$  across the chemocline is consistent with the process of microbial sulfate reduction;  
393 however, the sulfate concentrations also increased in the bottom waters (Figure 4), even when  
394 normalized to a conservative element such as chloride. The expected distillation pattern of  
395 sulfate consumption and increasing isotope composition of residual sulfate was not observed,  
396 and therefore precluded the calculation of fractionation factors using Rayleigh-type equations  
397 (e.g., Mariotti et al., 1981).

398  
399 The  $\delta^{34}\text{S}$  value of dissolved sulfide in the water column was  $-14.8\text{‰}$  at the oxic-anoxic interface  
400 and decreased to a minimum value of  $-25.1\text{‰}$  one meter below the chemocline (8 m, September  
401 2006, Figure 4). The isotopic composition of dissolved sulfide then increased progressively with  
402 depth by  $\sim 2\text{‰}$  above the sediment-water interface (12 to 13 m depth). The average isotopic  
403 offset at the chemocline ( $\Delta^{34}\text{S}_{\text{SO}_4\text{-H}_2\text{S}} = 37.1\text{‰}$ ), calculated as the difference between  $\delta^{34}\text{S}_{\text{SO}_4}$  and  
404  $\delta^{34}\text{S}_{\text{H}_2\text{S}}$ , increased with depth until 7.5 m ( $\Delta^{34}\text{S}_{\text{SO}_4\text{-H}_2\text{S}} = 51\text{‰}$ ), where it maintained a constant  
405 offset throughout the lower water column. The apparent fractionations are consistent with  
406 previous results of Overmann et al. (1996), which ranged from 49.4 to 55.5‰.

407

#### 408 *Sedimentary sulfur and pore waters in Mahoney Lake*

409 Solid-phase sulfur concentrations in sediments collected below the euxinic water mass (Cores 2  
410 and 3) were marginally higher than the sulfur content in a core collected above the chemocline  
411 (Core 9) (Table 2; Figure 5A). In Cores 2 and 3, AVS averaged  $0.26 \pm 0.06 \text{ wt.}\%$  ( $n = 29$ ),

412 compared to Core 9 concentrations of  $0.12 \pm 0.07$  wt.% ( $n = 15$ ). Downcore AVS was generally  
413 invariant within the anoxic cores relative to the subtle increase in concentrations toward the  
414 terminal depth of the oxic core. Pyrite-S concentrations (CRS) were higher in the anoxic cores  
415 ( $0.32 \pm 0.2$  wt.%,  $n = 19$ ) relative to the oxic core ( $0.04 \pm 0.01$  wt.%,  $n = 14$ ). There was a  
416 distinct pyrite maximum at 5.5 cm, followed by a near-linear decrease in concentrations within  
417 Core 2. The high degree of sulfurization ( $DOS > 0.7$ ) within Cores 2 and 3 positioned below the  
418 monimolimnion, including high values right at the sediment-water interface, is consistent with  
419 pyrite that formed in the euxinic water column or at the sediment-water interface (i.e., syngenetic  
420 pyrite). Mineral sulfide formation increased with sediment depth in oxic Core 9. Coincident with  
421 this increase, the DOS generally increased from a surficial value of 0.62 to 0.88 at the base of the  
422 core but with a distinct minimum of 0.28 at 9 cm. The high DOS values in Core 9 suggest past  
423 euxinic conditions at this presently oxic site (see discussion below).

424  
425 The concentrations and isotope values of sulfate in pore waters (Table 3) extracted from cores  
426 collected above and below the current position of the chemocline reflect the chemical  
427 composition of the overlying water. Specifically, interstitial sulfate concentrations in Cores 2  
428 and 3 ( $451.6 \pm 27$  mM) were similar to sulfate levels within the anoxic water column ( $426.7 \pm 53$   
429 mM). Likewise, within the oxic portion of the lake, Core 9 pore waters ( $300.1 \pm 7$  mM) were  
430 similar to those within the mixolimnion ( $353.8 \pm 44$  mM). The isotopic composition of pore  
431 water sulfate was nearly identical to the respective  $\delta^{34}\text{S}_{\text{SO}_4}$  and  $\delta^{18}\text{O}_{\text{SO}_4}$  of the oxic and anoxic  
432 bottom waters (Figure 5B). Although pore water sulfide concentrations were highly variable  
433 within Cores 2 and 3 ( $14.63 \pm 7$  mM), dissolved sulfide levels within Core 9 ( $1.66 \pm 0.4$  mM)  
434 were uniform and an order of magnitude lower than those within the euxinic cores (Table 3). The

435  $\delta^{34}\text{S}$  of pore water sulfide from Cores 2 and 3 ( $-22.1 \pm 2\%$ ) was consistent with that of bottom-  
436 water sulfide ( $-22.5 \pm 2.8\%$ ) (Figure 5B). Relative to the anoxic bottom waters, however, the  
437 isotopic composition of dissolved sulfide in Core 9 pore waters tended toward lower  $\delta^{34}\text{S}$  values,  
438 ranging from  $-17.9$  to  $-36.0\%$ .

439

#### 440 **4. Discussion**

##### 441 *Stable isotope spatial patterns and the Mahoney Lake sulfur supply*

442 The sulfur inventory of Mahoney Lake is exceptionally large, even when compared to both  
443 modern and ancient seawater. Water column sulfide ( $>30$  mM) is two orders of magnitude higher  
444 than concentrations measured in the deep waters of the Black Sea (Neretin et al., 2003), and the  
445 sulfate pool ( $>300$  mM) is tenfold greater than modern seawater. Although the source of sulfur  
446 has yet to be directly analyzed, Mahoney Lake sulfate is thought to be derived from the chemical  
447 dissolution of alkaline lavas (Northcote & Hall, 1983) in the western extent of the catchment  
448 (Marron Formation, Figure 1). The  $\delta^{34}\text{S}$  for such a source should fall near  $0\%$ , but intriguingly,  
449 the isotopic composition of sulfate in Mahoney Lake ( $\delta^{34}\text{S}_{\text{SO}_4} \approx 22\%$ ) is similar to that of  
450 modern seawater ( $\delta^{34}\text{S}_{\text{SO}_4} = 21\%$ ) (Rees, 1978). Equivalent values ( $\delta^{34}\text{S}_{\text{SO}_4} = 19.9\%$ ) were  
451 reported for drill-hole fluids (Michel et al., 2002) that infiltrate the White Lake Formation  
452 (composed of shale, sandstones, and volcanic conglomerates) 5 km to the northwest of the study  
453 area (Church, 2002).

454

455 The fault beneath both lakes (Figure 1) is a potential pathway for fluid flow into the catchment  
456 given that the overall geology of this region is highly fractured and favorable to basin-wide  
457 circulation of groundwater and hydrothermal fluids (Michels et al. 2002). Geothermal fluids

458 common to the region have characteristically high  $\delta^{18}\text{O}_{\text{H}_2\text{O}}$  (Magaritz & Taylor, 1986; Criss et  
459 al., 1991) (Figure 2, inset) and are unlikely sources of fluids because the lake water is very  
460 similar to meteoric inputs (Figure 2, LMWL). Long-term monitoring of lake levels further  
461 confirm that groundwater inflow is the dominant supply of water into Mahoney Lake (Northcote  
462 & Hall, 2000).

463  
464 The similarity between  $\delta^{34}\text{S}$  of the greenstone (0.8‰) and Sleeping Lake sulfate (1.6‰) suggests  
465 a sulfur source distinct from Mahoney Lake and Mahoney pond, which are both 20‰ higher and  
466 located less than 1 km away (Figure 1). The high  $\delta^{34}\text{S}_{\text{SO}_4}$  values in Mahoney Lake and the  
467 adjacent pond were derived either from a sulfur source from the western extent of the catchment  
468 or from a precursor sulfate similar to that of Sleeping Lake but that was heavily overprinted by  
469 isotopic fractionation during dissimilatory sulfate reduction. The Mahoney pond, perched above  
470 the lake, was observed to vary from a dry salt bed (2006) to a shallow pond (2008) during our  
471 two visits. Driving the sulfate pool to higher  $\delta^{34}\text{S}$  and  $\delta^{18}\text{O}$  in both an ephemeral pond and a  
472 persistent lake would require similar redox conditions and organic matter availability. However,  
473 climatic controls in the region suggest that the Mahoney pond likely remained dry for extended  
474 periods relative to the more stable water balance of Mahoney Lake. As such, sulfate pools in the  
475 two settings would evolve on different timescales and under different conditions, and therefore  
476 dissimilar  $\delta^{34}\text{S}$  and  $\delta^{18}\text{O}$  values should result. We are left with the likelihood that sulfate-rich  
477 waters in Mahoney Lake are delivered from weathering products derived from formations  
478 located to the west of the fault that bisects the catchment.

479

480 ***Water column stable isotope patterns***

481 Our study captured the steady-state isotopic variability ( $\delta^{34}\text{S}_{\text{SO}_4}$ ,  $\delta^{18}\text{O}_{\text{SO}_4}$ , and  $\delta^{34}\text{S}_{\text{H}_2\text{S}}$ ) of  
482 microbial processes within the Mahoney Lake water column during late summer to early fall. A  
483 turbidity maximum (Figure 3B) that coincides with the purple layer, the first appearance of  
484 dissolved sulfide, and near complete light attenuation, is proxy evidence for increased microbial  
485 biomass at the oxic-anoxic interface. The microbial plate (at 7 m) absorbs available light almost  
486 completely (Figure 3B), thus inhibiting further autotrophic production deeper in the water  
487 column.

488  
489 Microbial activity within the plate follows a seasonal pattern marked by peak productivity by  
490 purple sulfur bacteria during the late spring through early summer (Overmann et al., 1996).  
491 Through concomitant degradation of this biomass, sulfate reduction in the plate also becomes  
492 quantitatively important in late spring but extends through early fall (Overmann et al., 1991;  
493 Overmann et al., 1996). Primary production by purple sulfur bacteria is most intense at the top of  
494 the plate and is regulated by incoming solar radiation and the upward flux of dissolved sulfide  
495 transported from the monimolimnion (Overmann et al., 1991; Overmann et al., 1996). Mass  
496 balance estimates (Overmann et al., 1994; Overmann et al., 1996) as well as metagenomic data  
497 (Hamilton et al., 2014) indicate that chemoautotrophy is a significant sulfide oxidation pathway  
498 within the plate—in addition to anoxygenic photosynthesis.

499  
500 Comparison of rates of sulfate reduction (i.e., sulfide production) and anoxygenic photosynthetic  
501 productivity suggests that sulfate reduction is carbon-limited (Overmann et al., 1991; Overmann  
502 et al., 1996; Hamilton et al., 2014). Measured rates of carbon fixation and heterotrophic activity  
503 reveal that the carbon demand by sulfate reducers is greater than the amount of carbon fixed

504 during the summer; however, annual fixation rates ( $33.5 \text{ g C m}^{-2} \text{ yr}^{-1}$ ) are sufficient to satisfy the  
505 demand of sulfate reducers within the microbial plate ( $22.5 \text{ g C m}^{-2} \text{ yr}^{-1}$ ) (Overmann et al., 1996).  
506 Details of the extant microbial community were further refined by a recent study of 16s rRNA  
507 genes, which demonstrated that the Mahoney sulfur cycle is mediated by phototrophic sulfide  
508 oxidizers and oxidation of sulfide and intermediates by Epsilonproteobacteria and  
509 Deltaproteobacteria at the chemocline (7m) (Klepac-Ceraj et al., 2012). Microbiological  
510 evidence was also observed for sulfate reducers throughout the monimolimnion and within the  
511 sediments (Klepac-Ceraj et al., 2012; Hamilton et al., 2014). Although direct measurements of  
512 sulfate reduction rates and biomass enumerations are needed to determine the relative roles of  
513 these microorganisms, the genetic data confirm the activity of sulfate reducers within the lower  
514 water column and the sediments.

515  
516 The co-occurring processes of microbial sulfide production and sulfide oxidation provide a  
517 unique opportunity to study sulfur redox chemistry in a highly sulfidic natural system. Isotope  
518 patterns of sulfate and sulfide indicate active sulfate reduction at the oxic-anoxic interface in the  
519 water column (Figure 4). In our study, rapid increases in  $\delta^{34}\text{S}_{\text{SO}_4}$  ( $\sim 5\%$ ) and  $\delta^{18}\text{O}_{\text{SO}_4}$  ( $\sim 3\%$ )  
520 stabilized to constant values within the first 0.5 m below the chemocline. The relatively uniform  
521 sulfur isotope values for the sulfide in the deeper monimolimnion also increased at the  
522 chemocline by 7 to 9.5%. These isotope patterns are best explained by a combination of  
523 fractionations that occur during sulfate reduction and sulfide oxidation.

524  
525 Initial experiments with laboratory cultures suggested that the isotope effect that accompanies  
526 dissimilatory sulfate reduction produces offsets between sulfate and sulfide ( $\Delta^{34}\text{S}_{\text{SO}_4\text{-H}_2\text{S}}$ ) of up to

527 ~46‰ (Kaplan & Rittenberg, 1964b; Chambers et al., 1975) and that these results may reflect the  
528 maximum fractionations possible by sulfate reduction alone in the lab or natural settings  
529 (Canfield, 2001). However, recent culture experiments (Sim et al., 2011; Leavitt et al., 2013)  
530 and work in natural environments (Canfield et al., 2010) demonstrate fractionations of 60-70‰  
531 for sulfate reduction alone. Metabolic models for sulfate uptake followed by a series of  
532 enzymatic reduction steps within the cell that reduce sulfite and ultimately excrete sulfide (Rees,  
533 1973) may under-predict the magnitude of fractionation found in the natural environment (65-  
534 70‰) (Rudnicki et al., 2001; Wortmann et al., 2001). Brunner and Bernasconi (2005) reassessed  
535 biochemical pathways and fractionation effects that accompany reduction of sulfite to sulfide via  
536 the trithionate pathway and extended the potential fractionations up to 70‰. Network reaction  
537 models that incorporated multiple sulfur isotopes ( $^{32}\text{S}$ ,  $^{33}\text{S}$ ,  $^{34}\text{S}$ , and  $^{36}\text{S}$ ) (Farquhar et al., 2003;  
538 Farquhar et al., 2007; Johnston et al., 2007) improved the ability to model internal sulfur  
539 transformations, yet the relevant consequences of the enzyme dissimilatory sulfite reductase,  
540 which catalyzes the reduction of sulfite to sulfide, remain to be fully explored and understood  
541 (Bradley et al., 2011). The models discussed above establish the theoretical constraints on sulfur  
542 isotope effects during sulfate reduction, but the full expression of  $\delta^{34}\text{S}$  fractionation may also  
543 reflect environmental variables such as sulfate reduction rates (Kaplan & Rittenberg, 1964a;  
544 Kemp & Thode, 1968), carbon substrate (Aharon & Fu, 2000; Bolliger et al., 2001; Detmers et  
545 al., 2001), environmental conditions and microbial community structure (Brüchert et al., 2001;  
546 Detmers et al., 2001), and the size of the sulfate reservoir (Harrison & Thode, 1958; Habicht et  
547 al., 2002).

548



549 The oxidative sulfur cycle may further expand the isotopic difference between sulfate and  
550 sulfide. The presence of dissolved oxygen and purple sulfur bacteria at the redox interface of  
551 Mahoney Lake promotes abiotically and biotically mediated sulfide oxidation. However, sulfur  
552 isotope effects associated with sulfide oxidation are small ( $\pm 5\%$ ). For example, direct chemical  
553 oxidation of aqueous sulfide with molecular oxygen can increase  $\delta^{34}\text{S}_{\text{H}_2\text{S}}$  by  $5\%$  (Fry et al.,  
554 1988b), and purple sulfur bacteria typically produce residual  $\delta^{34}\text{S}_{\text{H}_2\text{S}}$  that is 2-5% lower than the  
555 product sulfate (Fry et al., 1984; Fry, 1986; Fry et al., 1988a; Zerkle et al., 2009; Zerkle et al.,  
556 2010; Brabec et al., 2012). Much larger fractionations are expected for sulfur disproportionation.  
557 For example, the simultaneous oxidation and reduction of sulfite produces  $^{34}\text{S}$ -enriched sulfate  
558 (7-12%) and  $^{34}\text{S}$ -depleted sulfide (20-37%) (Habicht et al., 1998). Combined transformations of  
559 reduction, reoxidation, and disproportionation have been invoked to explain large net isotopic  
560 offsets between sulfate and sulfide (Canfield & Thamdrup, 1994), particularly if the redox cycle  
561 is repeated multiple times.

562  
563 Chemical (Zhang & Millero, 1994) and microbial (Zopfi et al., 2001) sulfide oxidation at the  
564 chemocline generates intermediate sulfur compounds ( $\text{S}^0$ ,  $\text{SO}_3^{2-}$ ,  $\text{S}_2\text{O}_3^{2-}$ ) that can undergo  
565 disproportionation; however, biological and environmental conditions in Mahoney Lake  
566 potentially preclude or limit disproportionation to a very narrow zone within the uppermost  
567 portion of the chemocline. For example, purple sulfur bacteria oxidize sulfide directly to  
568 elemental sulfur, producing only very low levels of thiosulfate in Mahoney Lake ( $<1 - 20 \mu\text{M}$ )  
569 — levels that can inhibit thiosulfate disproportionation (Overmann et al., 1996). Furthermore, the  
570 high sulfide levels within the monimolimnion, well in excess of the sulfide tolerance ( $\sim 1 \text{ mM}$ )  
571 for either elemental sulfur or thiosulfate disproportionators (Thamdrup et al., 1993), likely

572 restricts disproportionators to the upper-cm of the chemocline. That said, the spatial resolution of  
573 our sampling methods (10 to 100 cm) might not capture the microbial signatures or specific  
574 chemical conditions at the top of the sulfide interface where sulfur disproportionating organisms  
575 could be active.

576  
577 The microbial process of sulfate reduction and associated rates appear to be to have the greatest  
578 influence on the isotopic patterns observed in this hyper-euxinic lake. The apparent fractionation  
579 between sulfate and sulfide (37.1 to 39.5‰) at the chemocline increased to 51‰ in water layers  
580 below the chemocline and remained fairly uniform throughout the monimolimnion (Figure 6).  
581 Consistent with previous results from Mahoney that ranged from 49 to 55‰ for coeval sulfate  
582 and sulfide sampled at the chemocline and 12 m water depth (Overmann et al., 1996), our data  
583 expand the vertical resolution and capture the increase in  $\delta^{34}\text{S}_{\text{H}_2\text{S}}$  values at the chemocline. The  
584 isotopic offset between oxidized and reduced sulfur in Mahoney Lake is similar to the large  
585 fractionations reported for euxinic marine water columns such as in the Black Sea, Cariaco  
586 Basin, Framvaren Fjord, Mariager Fjord, and the Orca Basin (Sweeney & Kaplan, 1980; Sheu et  
587 al., 1988; Fry et al., 1991; Mandernack et al., 2003; Neretin et al., 2003; Sørensen & Canfield,  
588 2004; Li et al., 2010), as well as euxinic lakes such as Lake Cadagno, Crawford Lake, and  
589 Fayetteville Green Lake (Deevey et al., 1963; Fry, 1986; Dickman & Thode, 1990; Canfield et  
590 al., 2010; Zerkle et al., 2010). Mahoney Lake has the highest concentrations of dissolved sulfide  
591 (>30 mM) and sulfate (> 300 mM) among these stratified water bodies. The large, effectively  
592 infinite sulfate reservoir in Mahoney Lake would preclude significant reservoir effects during  
593 sulfate reduction. When all these observations are considered, our favored interpretation is that  
594 large fractionations are dominantly instantaneous, occurring via sulfate reduction alone without

595 contributions from disproportionation in the sediment and water column. For these reasons,  
596 sulfate reduction exerts the greatest control on  $\delta^{34}\text{S}$  fractionation in Mahoney Lake.

597  
598 Paired  $\delta^{34}\text{S}_{\text{SO}_4}$  and  $\delta^{18}\text{O}_{\text{SO}_4}$  data offer an additional constraint on the microbial redox cycle within  
599 Mahoney Lake. The low temperature and near-neutral pH of the Mahoney water column  
600 measured during our studies (pH 7-9, 9-24°C), as well as during long-term monitoring  
601 (Northcote & Halsey, 1969; Northcote & Hall, 1983), suggest that sulfate-oxygen has not  
602 undergone abiotic equilibrium exchange and thus records biogenic oxygen isotope effects. Under  
603 anoxic conditions, sulfate-oxygen can fractionate during sulfate reduction, and the extent of  
604 enrichment is controlled by kinetic isotope effects imparted during intracellular enzymatic steps  
605 and/or equilibrium oxygen exchange with water. Mizutani and Rafter (1969) proposed a 1:4  
606 ( $\delta^{18}\text{O}_{\text{SO}_4}:\delta^{34}\text{S}_{\text{SO}_4} = 0.25$ ) kinetic relationship between the  $\delta^{34}\text{S}$  and  $\delta^{18}\text{O}$  of sulfate based on an  
607 assumption of preferential  $^{16}\text{O}$ -bond rupture and the stoichiometry of the sulfate molecule. The  
608 theoretical  $\delta^{18}\text{O}_{\text{SO}_4}:\delta^{34}\text{S}_{\text{SO}_4}$  slope of 0.25 suggests the  $\delta^{34}\text{S}$  and  $\delta^{18}\text{O}$  of residual sulfate evolves in  
609 a linear relationship during sulfate reduction; however, studies of natural samples tend to reveal a  
610 curvilinear response that implies equilibrium isotope exchange regulates the oxygen isotope  
611 composition of residual sulfate (Böttcher et al., 1998; Brunner et al., 2005; Brunner et al., 2012;  
612 Antler et al., 2013). Culturing experiments and reactive transport models of natural samples point  
613 to oxygen isotope exchange between water and metabolic intermediates (APS, AMP, and sulfite)  
614 that buffers the  $\delta^{18}\text{O}_{\text{SO}_4}$  to a maximum value determined by the ambient  $\delta^{18}\text{O}_{\text{H}_2\text{O}}$  value and  
615 associated fractionation factors (Mizutani & Rafter, 1973; Fritz et al., 1989; Brunner et al., 2005;  
616 Knöller et al., 2006; Wortmann et al., 2007; Turchyn et al., 2010). The combined effects of  
617 Rayleigh-type kinetic isotope fractionations and oxygen isotope exchange during sulfate

618 reduction thus results in non-linear  $\delta^{18}\text{O}$ - $\delta^{34}\text{S}$  arrays. In studies of marine pore waters, sulfate  
619 approaches a plateau in  $\delta^{18}\text{O}_{\text{SO}_4}$ , in apparent equilibrium with seawater, as  $\delta^{34}\text{S}_{\text{SO}_4}$  evolves  
620 toward higher values (Zak et al., 1980; Böttcher et al., 1998; Blake et al., 2006; Riedinger et al.,  
621 2010; Wehrmann et al., 2011; Antler et al., 2013). Empirical equations based on high  
622 temperature exchange experiments between sulfate and water (Lloyd, 1968; Mizutani, 1972) and  
623 quantum mechanical calculations (Zeebe, 2010) can constrain the  $\delta^{18}\text{O}_{\text{SO}_4}$  value in equilibrium  
624 with ambient water. These relationships (Lloyd, 1968; Mizutani, 1972; Zeebe, 2010) yield  
625 apparent equilibrium  $\delta^{18}\text{O}_{\text{SO}_4}$  values ranging between 24 to 36‰ for the temperature and isotopic  
626 composition of anoxic water (about 9°C and -2‰) in Mahoney Lake. These equilibrium values  
627 overestimate the observed  $\delta^{18}\text{O}_{\text{SO}_4}$  by 3 to 15‰.

628  
629 Instead, we observe near-linear patterns of  $\delta^{18}\text{O}_{\text{SO}_4}$  and  $\delta^{34}\text{S}_{\text{SO}_4}$  in the water columns sampled in  
630 fall and summer (Figure 7), which is a trend more consistent with high sulfate reduction rates  
631 than equilibrium isotope exchange (Böttcher et al., 1998; Brunner & Bernasconi, 2005; Brunner  
632 et al., 2012; Antler et al., 2013). The model arrays represent a range of possible solutions for the  
633 internal cycling of sulfur during microbial sulfate reduction (Figure 7). Steep slopes (Figure 7A,  
634 Trend B) with large changes in  $\delta^{18}\text{O}_{\text{SO}_4}$  relative to those in  $\delta^{34}\text{S}_{\text{SO}_4}$  are consistent with lower rates  
635 of sulfate reduction and enhanced recycling of intracellular sulfur (Antler et al., 2013).  
636 Conversely, low-angle slopes (Figure 7A, Trend A) with little change in  $\delta^{18}\text{O}_{\text{SO}_4}$  over large  
637 changes in  $\delta^{34}\text{S}_{\text{SO}_4}$  are observed in systems with rapid sulfate reduction rates and minimal  
638 recycling of intracellular sulfur (Antler et al., 2013).

639

640 In addition to the behavior in  $\delta^{18}\text{O}_{\text{SO}_4}$ - $\delta^{34}\text{S}_{\text{SO}_4}$ , the extent of instantaneous fractionation between  
641 water column sulfate and sulfide lends support to our interpretation of high sulfate reduction  
642 rates in Mahoney Lake. It is well demonstrated that sulfur isotope fractionation factors are  
643 inversely proportional to the rates of sulfate reduction (Sim et al., 2011; Leavitt et al., 2013),  
644 which is in turn dependent on the availability and reactivity of organic matter (e.g., Overmann,  
645 1997; Hamilton et al., 2014). We observed sulfide with high  $\delta^{34}\text{S}$  (-14.8‰) and the smallest  
646 isotopic offset between sulfate and sulfide (37.1‰) at the chemocline (Figure 6), which may  
647 reflect the rapid rates of sulfate reduction in that portion of the water column. The increase in  
648  $\delta^{18}\text{O}_{\text{SO}_4}$  and  $\delta^{34}\text{S}_{\text{SO}_4}$  thus depends on the localized activity of sulfate reducers. The process of  
649 microbial sulfate reduction may occur at the redoxcline in the water column, throughout the  
650 water column, and possibly in the sediments as well. The anoxic basins of the Black Sea and  
651 Cariaco Basin serve as templates for recognizing such hotspots of microbial activity. Sulfate  
652 reduction rates measured in the Black Sea revealed distinct zones of sulfate reduction within the  
653 chemocline and at the sediment-water interface (Albert et al., 1995). Volumetrically, the rates of  
654 sulfate reduction within the sediments of the Black Sea are three-fold greater than those within  
655 the water column, suggesting that much of the sulfide in the water column is delivered via  
656 diffusion from sulfate reduction in the sediments (Albert et al., 1995). Similar zones and modes  
657 of sulfide production are postulated for the Caricaco Basin (Fry et al., 1991; Li et al., 2010). The  
658 microbial diversity of Mahoney Lake suggests that sulfate reducing bacteria are distributed  
659 throughout the anoxic water column and sediments (Hamilton et al., 2014). The near-linear  
660 isotope arrays for sulfate with  $\delta^{18}\text{O}_{\text{SO}_4}$ : $\delta^{34}\text{S}_{\text{SO}_4}$  slopes ranging between 0.47 (July 2008;  $R^2 =$   
661 0.94) and 0.60 (September 2006;  $R^2 = 0.96$ ) (Figure 7) are consistent with high sulfate reduction  
662 rates in the water column.

663  
664 It is intriguing that the slope shifts from low values in the summer (Figure 7C) to higher values  
665 in fall (Figure 7B). The shallower  $\delta^{18}\text{O}_{\text{SO}_4}:\delta^{34}\text{S}_{\text{SO}_4}$  slope in the summer implies sulfate reduction  
666 rates that are relatively higher than those in the fall. Overmann et al. (1996) observed that sulfate  
667 reduction rates peak during the summer after the spring bloom of purple sulfur bacteria, and then  
668 decrease in the fall as photosynthetic activity diminishes. Labile organic acids released from the  
669 degradation of purple sulfur bacteria provide the primary carbon substrate mineralized by sulfate  
670 reducers (Overmann et al., 1996). Previous studies demonstrate that linear  $\delta^{18}\text{O}_{\text{SO}_4}:\delta^{34}\text{S}_{\text{SO}_4}$  slopes  
671 are sensitive to the quantity and reactivity of organic matter mineralized during sulfate reduction  
672 (Aharon & Fu, 2000; Antler et al., 2014). The change in the  $\delta^{18}\text{O}_{\text{SO}_4}:\delta^{34}\text{S}_{\text{SO}_4}$  slope of residual  
673 sulfate reported here thus may track the seasonal activity of sulfate reduction stimulated by the  
674 localized primary productivity of anoxygenic phototrophs within the plate. Dedicated seasonal  
675 sampling may capture a more robust isotopic signature of evolving sulfate reduction rates.  
676 Likewise, our modeled data could be re-evaluated as separate but coupled trajectories for the  
677 chemocline and deeper sulfide production within the bottom waters and surficial sediments;  
678 however, the current data set lacks the spatial resolution to make this determination. The  
679 potentially distinct zones and rates of reduction might be revealed within higher resolution  
680  $\delta^{18}\text{O}_{\text{SO}_4}$  and  $\delta^{34}\text{S}_{\text{SO}_4}$  data collected at the sub-cm scale.

681  
682 Close inspection of the isotope variability near the chemocline does reveal that  $\delta^{18}\text{O}_{\text{SO}_4}$  varies  
683 more than  $\delta^{34}\text{S}_{\text{SO}_4}$  (Figure 7A). The 2-3‰ increase in  $\delta^{18}\text{O}_{\text{SO}_4}$  and lack of response in  $\delta^{34}\text{S}_{\text{SO}_4}$   
684 implies sulfate reduction and near quantitative reoxidation to sulfate (i.e., no net sulfur isotope  
685 fractionation). Oxygen isotope fraction during disproportionation can be large (up to 21‰)

686 (Böttcher et al., 2001) and therefore do not agree with the smaller isotope effects observed here,  
687 consistent with our earlier arguments against appreciable disproportionation. Below 7 m water  
688 depth, both  $\delta^{18}\text{O}_{\text{SO}_4}$  and  $\delta^{34}\text{S}_{\text{SO}_4}$  follow a sulfate reduction trend of increasing values. Therefore,  
689 although there is clear evidence for robust activity of sulfur oxidizing bacteria, the prevailing  
690 process of microbial sulfate reduction masks the isotopic fingerprint.

691  
692 We acknowledge that thermodynamic equilibrium can achieve large isotopic offsets ( $\sim 75\%$ )  
693 between sulfate and sulfide (Ohmoto & Lasaga, 1982; Chu et al., 2004; Farquhar et al., 2007;  
694 Johnston et al., 2007; Leavitt et al., 2014) in the absence of biological activity. The extremely  
695 high concentrations of aqueous sulfur compounds (including sulfate, sulfide, and polysulfide)  
696 within our study area makes Mahoney Lake a candidate system for the consideration of abiotic  
697 isotope fractionation. Equilibrium isotope exchange between sulfate-sulfide depends upon pH  
698 and temperature and can equilibrate within days under acidic conditions (pH = 2) and high  
699 temperature ( $>300^\circ\text{C}$ ) (Ohmoto & Lasaga, 1982). However, at normal Earth surface  
700 temperatures ( $25^\circ\text{C}$ ) and neutral pH, near quantitative exchange (90%) between aqueous sulfate  
701 and sulfide is exceedingly slow, taking on the order of  $10^9$  years (Ohmoto & Lasaga, 1982),  
702 which is well in excess of the age of Mahoney Lake ( $10^4$  years). The proposed mechanism for  
703 sulfate-sulfide exchange may occur through a transient thiosulfate intermediate (Ohmoto &  
704 Lasaga, 1982) or polysulfides (Chu et al., 2004); however, controlled experiments needed to  
705 further constrain these processes remain to be conducted. One recent study shows that sulfur  
706 isotope exchange may be possible during thiosulfate disproportionation but mass balance  
707 considerations suggest that the isotope effects are kinetic (Leavitt et al., 2014). Based on the

708 current understanding of the sulfate-sulfide system, the isotope offsets in Mahoney Lake are thus  
709 most consistent with biologically mediated sulfur cycling.

710

### 711 *Linking the pelagic S cycle with the sedimentary record*

712 The large size of the sulfate and sulfide reservoir defines the isotopic composition of the pore  
713 waters within both the oxygenated (Core 9) and the anoxic (Cores 2 and 3) portions of the lake.

714 Pore water  $\delta^{34}\text{S}_{\text{SO}_4}$  and  $\delta^{18}\text{O}_{\text{SO}_4}$  values are identical to the isotopic compositions of sulfate from  
715 the mixolimnion or the monimolimnion (Figure 5B). Relative to Core 9 collected from the oxic  
716 margin of Mahoney Lake, pore waters in Cores 2 and 3 are  $^{34}\text{S}$ - and  $^{18}\text{O}$ -enriched. The  
717 comparatively higher  $\delta^{34}\text{S}_{\text{SO}_4}$  and  $\delta^{18}\text{O}_{\text{SO}_4}$  are likely driven by fractionations during sulfate  
718 reduction.

719

720  $\delta^{34}\text{S}_{\text{SO}_4}$  data for the water column and associated pore waters plot along mixing trajectories  
721 specific to the oxic and anoxic study sites (Figure 8A). Sulfate in the oxic water column has  
722 uniform  $\delta^{34}\text{S}_{\text{SO}_4}$  over a broad range of sulfate concentrations. Core 9 pore waters have  $\delta^{34}\text{S}_{\text{SO}_4}$   
723 values identical to those of the mixolimnion. Sulfate in the anoxic water column becomes  $^{34}\text{S}$ -  
724 enriched as sulfate concentrations increase with depth. Pore waters all have high sulfate  
725 concentrations with high  $\delta^{34}\text{S}$  values. Mixing patterns in  $\delta^{18}\text{O}_{\text{SO}_4}$  (Figure 8B) show similar  
726 trends, albeit with greater scatter in the isotope data. Although the sulfate concentrations within  
727 the pore waters remain high and the sulfate isotope data follow patterns of mixing, the pore water  
728  $\delta^{34}\text{S}_{\text{H}_2\text{S}}$  values in the oxic margin (Core 9) are highly variable (Figure 6) and decrease depth  
729 (Figure 5B), indicating active sulfide production within the sediments. As discussed above, the  
730 activity of sulfate reduction within the plate appears to be tied to the productivity of purple sulfur



731 bacteria, this relationship does not preclude the burial of reactive organic compounds that  
732 escaped oxidation in the water column.

733  
734 The dissolved sulfide pool is also large within the monimolimnion and the pore waters within  
735 Cores 2 and 3. Similarity between  $\delta^{34}\text{S}_{\text{H}_2\text{S}}$  in the water column and the pore waters suggests that  
736 isotopic compositions are buffered by the large sulfide concentrations within the euxinic water  
737 mass (Figure 5B). The concentrations of sedimentary dissolved sulfide, AVS, and pyrite beneath  
738 the euxinic waters are appreciable relative to those in the sediments of the oxic margin. The  $\delta^{34}\text{S}$   
739 of pyrite, within our small errors, is the same as the composition of water column sulfide (Figure  
740 5A). High DOS values ( $\sim 0.8$ ) within Cores 2 and 3 suggest water column pyrite synthesis within  
741 a euxinic water column. Although the data suggest that pyrite formation is ultimately Fe limited,  
742 the high DOS values also suggest that an iron enrichment mechanism perhaps like that observed  
743 in the modern Black Sea (e.g., Lyons & Severmann, 2006) may be operating in the lake.

744  
745 Seasonal recycling by reductive dissolution and oxidation may transport iron into the deeper lake  
746 from the oxic margin; however, a benthic shallow-to-deep iron flux at the small scale of this  
747 basin has yet to be described elsewhere. The low and invariant  $\delta^{34}\text{S}$  of pyrite within both anoxic  
748 cores further supports our interpretation of water column pyrite formation (Lyons, 1997; Lyons  
749 et al., 2003). In contrast, pore water sulfide in Core 9 becomes more  $^{34}\text{S}$ -depleted with depth, and  
750 AVS accumulates with depth, implying sulfide generation in the sediments. The DOS values  
751 within the upper 15 cm of the sediment column also increase down core, consistent with  
752 diagenetic pyrite formation, and eventually reach high values more typical of water-column  
753 pyrite formation in the euxinic part of the basin (0.8). A shoaling of the chemocline when water

754 levels were higher likely explains the down-core transition to higher DOS in the now oxic core.  
755 Modern observations show the lake experiences long-term volumetric changes. Lake level has  
756 dropped more than 5 m since 1961 (Northcote & Hall, 1990; Northcote & Hall, 2000; Northcote  
757 & Hall, 2010). Decadal fluctuations in lake height potentially control the vertical position of the  
758 chemocline and thus the expansion (when lake levels are high) or contraction (when lake levels  
759 are low) of the volume of the euxinic bottom waters. The lateral displacement of the chemocline  
760 from depo-center to margin, as tracked by excursions in DOS, may coincide with regional  
761 drought. Shoaling events are well documented for the Black Sea (Lyons et al., 1993) and, in  
762 Mahoney, are likely caused by changing lake volume.

763

#### 764 *Long-term stability of the chemocline*

765 The dissolved sulfide concentrations of  $>30$  mM are considerable and represent extreme euxinic  
766 conditions. Very high sulfide concentrations within the anoxic bottom waters are consistent with  
767 previous reports (Northcote & Halsey, 1969; Northcote & Hall, 1983); however, we also  
768 detected free sulfide at isolated depths in the mixolimnion at concentrations ranging 3 to 62  $\mu$ M  
769 (Table 1, Figure 3). The low but analytically detectable sulfide levels ( $> 2$   $\mu$ M) may reflect  
770 sulfide released from aggregates of purple sulfur bacteria transported into the oxic surface waters  
771 by wind-blown mixing. During both field trips, we observed aggregates of purple sulfur bacteria  
772 floating within the mixolimnion and deposited along the shoreline. Overmann *et al.* (1994)  
773 reported that the majority of purple sulfur bacteria were photosynthetically inactive during late  
774 summer, and approximately 86% of the biomass was dispersed from the plate into the upper  
775 water column.

776

777 Redox instability is part of the history of Mahoney Lake. Paleoreconstructions suggest anoxic  
778 conditions commenced with the formation of Mahoney Lake following glacial retreat 11,000  
779 years ago. Diatom and midge sediment archives record elevated salinities (~10 g/L) throughout  
780 much of the Holocene (Heinrichs et al., 1997) and imply that aridity is a persistent feature of the  
781 regional climate. Okenone abundances indicate several purple sulfur bacteria blooms and periods  
782 of meromixis lasting approximately 1000 years (Overmann et al., 1993; Coolen & Overmann,  
783 1998). The periodicity found in purple sulfur biomarkers is consistent with the absence of  
784 laminations during low stands and implies that wind-driven mixing destabilized the stratification  
785 (Dickman, 1985; Lowe et al., 1997).

786

## 787 **5. Conclusions**

788 We studied the isotope composition of sulfate and sulfide within the water column and sediments  
789 of a hyper-euxinic lake. Our analysis of surface water samples collected from four lakes located  
790 within the same catchment indicates that the sulfate in Mahoney Lake is derived from rock units  
791 in the western portion of the watershed. The sulfate (>300 mM) and sulfide (>30 mM)  
792 concentrations in the Mahoney Lake water column are extremely high and unlike sulfur  
793 inventories postulated for the Proterozoic and Archean oceans; however, the sulfide availability  
794 within the photic zone coupled within a highly active microbial community of sulfate reducing  
795 and sulfur phototrophic bacteria provide an ideal natural laboratory for studying biological  
796 processes thought to be prevalent in euxinic seas. Our data revealed that although there is clearly  
797 a very active plate of purple sulfur bacteria, the associated isotopic biosignature is completely  
798 overprinted by the relatively large sulfur and oxygen isotope fractionations associated with  
799 sulfate reducing bacteria. The seasonal  $\delta^{18}\text{O}_{\text{SO}_4}$ - $\delta^{34}\text{S}_{\text{SO}_4}$  patterns observed in water column

800 suggest that sulfate reduction rates (low  $\delta^{18}\text{O}_{\text{SO}_4}:\delta^{34}\text{S}_{\text{SO}_4}$  slope) are high during the summer and  
801 decrease in the fall (high  $\delta^{18}\text{O}_{\text{SO}_4}:\delta^{34}\text{S}_{\text{SO}_4}$  slope). The decrease in the offset between sulfate and  
802 sulfide ( $\Delta^{34}\text{S}_{\text{SO}_4\text{-H}_2\text{S}} = 37\text{‰}$ ) near the chemocline is also consistent with higher rates of sulfate  
803 reduction (and an associated decrease in fractionation at higher rates). Previous studies  
804 demonstrate that productivity of sulfate reducers is dependent upon carbon inputs from purple  
805 sulfur bacteria. Although the isotope signatures of sulfate reduction mask the relatively small  
806 isotope effects produced during sulfide oxidation, the linear correlation between  $\delta^{18}\text{O}_{\text{SO}_4}$  and  
807  $\delta^{34}\text{S}_{\text{SO}_4}$  is potentially influenced by the primary production of anoxygenic photosynthetic  
808 bacteria. As with the water column, the  $\delta^{34}\text{S}$  of sedimentary pyrite reflects the process of sulfate  
809 reduction. Estimates of the degree of sulfurization (DOS > 0.7) suggest that the deep basin  
810 sediments pyrites likely form in the water column and settle to the sediments. Although a  
811 mechanism for reactive iron delivery within a small basin such as Mahoney Lake has yet to be  
812 fully explored, the trend toward higher DOS within sediments collected from the oxic margin  
813 suggests lake level (and water availability) influences the expansion/contraction of the euxinic  
814 water mass.

815  
816 As a result of strong overprinting by microbial sulfate reduction, there is not an obvious stable  
817 isotope signature for photosynthetic sulfide oxidation in Mahoney Lake that could be  
818 incorporated into the sedimentary record. In effect, the isotopic expression of sulfate reduction  
819 integrated over the entire anoxic water column and under non-sulfate-limiting conditions masks  
820 the isotopic effects of phototrophic sulfide oxidation within the  $\delta^{18}\text{O}_{\text{SO}_4}\text{-}\delta^{34}\text{S}_{\text{SO}_4}$  system.  
821 However, there is clear evidence within seasonal response of  $\delta^{18}\text{O}_{\text{SO}_4}\text{-}\delta^{34}\text{S}_{\text{SO}_4}$  for extensive sulfur  
822 cycling through phototrophic sulfide oxidation in Mahoney Lake, suggesting that if the difficult

823 task of constraining ambient  $\delta^{18}\text{O}_{\text{H}_2\text{O}}$  (Brabec et al., 2012) can be surmounted (through, for  
824 example, combined clumped isotope paleothermometry and  $\delta^{18}\text{O}$  analysis of carbonate phases)  
825 the combined sulfur and oxygen isotope systematics of sedimentary sulfate may ultimately  
826 provide an archive of the prevalence and magnitude of photosynthetic sulfur cycling during  
827 Earth's history.

828

### 829 *Acknowledgements*

830 We thank BC Ministry of Environment Area Supervisors R. Gunoff and M. Weston for access to  
831 Mahoney Lake and their generous field support. S. Bates, A. Chappaz, A. Dekas, G. Druschel,  
832 D. Fike, B. Gill, J. Glass, M. McKibben, N. Planavsky, N. Riedinger, and A. Vossmeier assisted  
833 in the field or laboratory. Hydrolabs were provided by M. Anderson UCR, and LacCore  
834 (National Lacustrine Core Facility, Department of Geology and Geophysics, University of  
835 Minnesota-Twin Cities). The manuscript benefited from helpful discussions with K. Hall, T.  
836 Northcote, C. Alpers, K. Mandernack, and J. Overmann. We also thank D. Johnston and two  
837 anonymous reviewers for their thoughtful and constructive reviews. Funding for our research  
838 was provided by NASA Exobiology and the NASA Astrobiology Institute (TL), the American  
839 Chemical Society Petroleum Research Fund (48736-ND2 to TL and WPG), and an Agouron  
840 Institute Geobiology Fellowship (WPG).

841

### 842 **References**

843

844 Aharon P, Fu B (2000) Microbial sulfate reduction rates and sulfur and oxygen isotope  
845 fractionations at oil and gas seeps in deepwater Gulf of Mexico. *Geochimica et*  
846 *Cosmochimica Acta*, **64**, 233-246.

- 847 Albert DB, Taylor C, Martens CS (1995) Sulfate reduction rates and low molecular weight fatty  
848 acid concentrations in the water column and surficial sediments of the Black Sea. *Deep*  
849 *Sea Research Part I: Oceanographic Research Papers*, **42**, 1239-1260.
- 850 Antler G, Turchyn AV, Herut B, Davies A, Rennie VC, Sivan O (2014) Sulfur and oxygen  
851 isotope tracing of sulfate driven anaerobic methane oxidation in estuarine sediments.  
852 *Estuarine, Coastal and Shelf Science*, **142**, 4-11.
- 853 Antler G, Turchyn AV, Rennie V, Herut B, Sivan O (2013) Coupled sulfur and oxygen isotope  
854 insight into bacterial sulfate reduction in the natural environment. *Geochimica et*  
855 *Cosmochimica Acta*, **118**, 98-117.
- 856 Balci N, Mayer B, Shanks Iii WC, Mandernack KW (2012) Oxygen and sulfur isotope  
857 systematics of sulfate produced during abiotic and bacterial oxidation of sphalerite and  
858 elemental sulfur. *Geochimica et Cosmochimica Acta*, **77**, 335-351.
- 859 Balci N, Shanks WC, Iii, Mayer B, Mandernack KW (2007) Oxygen and sulfur isotope  
860 systematics of sulfate produced by bacterial and abiotic oxidation of pyrite. *Geochimica*  
861 *et Cosmochimica Acta*, **71**, 3796-3811.
- 862 Bekker A, Holland HD, Wang PL, Rumble D, Stein HJ, Hannah JL, Coetsee LL, Beukes NJ  
863 (2004) Dating the rise of atmospheric oxygen. *Nature*, **427**, 117-120.
- 864 Berner RA (1970) Sedimentary pyrite formation. *Am J Sci*, **268**, 1-23.
- 865 Blake RE, Surkov AV, Böttcher ME, Ferdelman TG, Jørgensen BB (2006) Oxygen isotope  
866 composition of dissolved sulfate in deep-sea sediments: eastern equatorial Pacific Ocean.  
867 In: *Proceedings of the Ocean Drilling Program, Scientific Results* (eds Jørgensen BB,  
868 D'hondt SL, Miller DJ), pp. 1-23.
- 869 Boesen C, Postma D (1988) Pyrite formation in anoxic environments of the Baltic. *Am J Sci*,  
870 **288**, 575-603.
- 871 Bolliger C, Schroth MH, Bernasconi SM, Kleikemper J, Zeyer J (2001) Sulfur isotope  
872 fractionation during microbial sulfate reduction by toluene-degrading bacteria.  
873 *Geochimica et Cosmochimica Acta*, **65**, 3289-3298.
- 874 Böttcher ME, Oelschläger B, Höpner T, Brumsack H-J, Rullkötter J (1998) Sulfate reduction  
875 related to the early diagenetic degradation of organic matter and "black spot" formation in  
876 tidal sandflats of the German Wadden Sea (southern North Sea): stable isotope ( $^{13}\text{C}$ ,  
877  $^{34}\text{S}$ ,  $^{18}\text{O}$ ) and other geochemical results. *Organic Geochemistry*, **29**, 1517-1530.
- 878 Böttcher ME, Thamdrup B, Vennemann TW (2001) Oxygen and sulfur isotope fractionation  
879 during anaerobic bacterial disproportionation of elemental sulfur. *Geochimica et*  
880 *Cosmochimica Acta*, **65**, 1601-1609.
- 881 Bottrell SH, Newton RJ (2006) Reconstruction of changes in global sulfur cycling from marine  
882 sulfate isotopes. *Earth-Science Reviews*, **75**, 59-83.
- 883 Brabec MY, Lyons TW, Mandernack KW (2012) Oxygen and Sulfur Isotope Fractionation  
884 during Sulfide Oxidation by Anoxygenic Phototrophic Bacteria. *Geochimica et*  
885 *Cosmochimica Acta*, **83**, 234-251.
- 886 Bradley AS, Leavitt WD, Johnston DT (2011) Revisiting the dissimilatory sulfate reduction  
887 pathway. *Geobiology*, **9**, 446-457.
- 888 Brocks JJ, Love GD, Summons RE, Knoll AH, Logan GA, Bowden SA (2005) Biomarker  
889 evidence for green and purple sulphur bacteria in a stratified Palaeoproterozoic sea.  
890 *Nature*, **437**, 866-870.

- 891 Brocks JJ, Schaeffer P (2008) Okenane, a biomarker for purple sulfur bacteria (Chromatiaceae),  
892 and other new carotenoid derivatives from the 1640 Ma Barney Creek Formation.  
893 *Geochimica et Cosmochimica Acta*, **72**, 1396-1414.
- 894 Brüchert V, Knoblauch C, Jørgensen BB (2001) Controls on stable sulfur isotope fractionation  
895 during bacterial sulfate reduction in Arctic sediments. *Geochimica et Cosmochimica*  
896 *Acta*, **65**, 763-776.
- 897 Brunner B, Bernasconi SM (2005) A revised isotope fractionation model for dissimilatory sulfate  
898 reduction in sulfate reducing bacteria. *Geochimica et Cosmochimica Acta*, **69**, 4759-  
899 4771.
- 900 Brunner B, Bernasconi SM, Kleikemper J, Schroth MH (2005) A model for oxygen and sulfur  
901 isotope fractionation in sulfate during bacterial sulfate reduction processes. *Geochimica*  
902 *et Cosmochimica Acta*, **69**, 4773-4785.
- 903 Brunner B, Einsiedl F, Arnold GL, Müller I, Templer S, Bernasconi SM (2012) The reversibility  
904 of dissimilatory sulphate reduction and the cell-internal multi-step reduction of sulphite  
905 to sulphide: insights from the oxygen isotope composition of sulphate. *Isotopes in*  
906 *environmental and health studies*, **48**, 33-54.
- 907 Calmels D, Gaillardet J, Brenot A, France-Lanord C (2007) Sustained sulfide oxidation by  
908 physical erosion processes in the Mackenzie River basin: Climatic perspectives. *Geology*,  
909 **35**, 1003-1006.
- 910 Canfield DE (1998) A new model for Proterozoic ocean chemistry. *Nature*, **396**, 450-453.
- 911 Canfield DE (2001) Biogeochemistry of Sulfur Isotopes. In: *Stable Isotope Geochemistry* (eds  
912 Valley JW, Cole DR). Mineralogical Society of America, Washington DC, pp. 607-636.
- 913 Canfield DE, Farquhar J (2009) Animal evolution, bioturbation, and the sulfate concentration of  
914 the oceans. *Proceedings of the National Academy of Sciences*, **106**, 8123-8127.
- 915 Canfield DE, Farquhar J, Zerkle AL (2010) High isotope fractionations during sulfate reduction  
916 in a low-sulfate euxinic ocean analog. *Geology*, **38**, 415-418.
- 917 Canfield DE, Raiswell R, Westrich JT, Reaves CM, Berner RA (1986) The use of chromium  
918 reduction in the analysis of reduced inorganic sulfur in sediments and shales. *Chemical*  
919 *Geology*, **54**, 149-155.
- 920 Canfield DE, Teske A (1996) Late Proterozoic rise in atmospheric oxygen concentration inferred  
921 from phylogenetic and sulphur-isotope studies. *Nature* **382**, 127-132.
- 922 Canfield DE, Thamdrup B (1994) The Production of <sup>34</sup>S-Depleted Sulfide During Bacterial  
923 Disproportionation of Elemental Sulfur. *Science*, **266**, 1973-1975.
- 924 Chambers LA, Trudinger PA, Smith JW, Burns MS (1975) Fractionation of sulfur isotopes by  
925 continuous cultures of *Desulfovibrio desulfuricans*. *Canadian Journal of Microbiology*,  
926 **21**, 1602-1607.
- 927 Chanton J, Martens C (1985) The effects of heat and stannous chloride addition on the active  
928 distillation of acid volatile sulfide from pyrite-rich marine sediment samples.  
929 *Biogeochemistry*, **1**, 375-382-382.
- 930 Chiba H, Sakai H (1985) Oxygen isotope exchange rate between dissolved sulfate and water at  
931 hydrothermal temperatures. *Geochimica et Cosmochimica Acta*, **49**, 993-1000.
- 932 Chu X, Ohmoto H, Cole DR (2004) Kinetics of sulfur isotope exchange between aqueous sulfide  
933 and thiosulfate involving intra- and intermolecular reactions at hydrothermal conditions.  
934 *Chemical Geology*, **211**, 217-235.
- 935 Church BN (2002) Geoscience Map 2002-5: Geology of the Penticton Tertiary Outlier, British  
936 Columbia (NTS 082E/5).

- 937 Claypool GE, Holser WT, Kaplan IR, Sakai H, Zak I (1980) The age curves of sulfur and oxygen  
938 isotopes in marine sulfate and their mutual interpretation. *Chemical Geology*, **28**, 199-  
939 260.
- 940 Cline JD (1969) Spectrophotometric Determination of Hydrogen Sulfide in Natural Waters.  
941 *Limnology and Oceanography*, **14**, 454-458.
- 942 Coolen MJL, Overmann J (1998) Analysis of Subfossil Molecular Remains of Purple Sulfur  
943 Bacteria in a Lake Sediment. *Applied and Environmental Microbiology*, **64**, 4513-4521.
- 944 Cornwell JC, Morse JW (1987) The characterization of iron sulfide minerals in anoxic marine  
945 sediments. *Marine Chemistry*, **22**, 193-206.
- 946 Criss RE, Fleck RJ, Taylor HP (1991) Tertiary Meteoric Hydrothermal Systems and their  
947 Relation to Ore Deposition, Northwestern United States and Southern British Columbia.  
948 *Journal of Geophysical Research*, **96**, 13,335-313,356.
- 949 Crowe SA, Paris G, Katsev S, Jones C, Kim S-T, Zerkle AL, Nomosatryo S, Fowle DA, Adkins  
950 JF, Sessions AL, Farquhar J, Canfield DE (2014) Sulfate was a trace constituent of  
951 Archean seawater. *Science*, **346**, 735-739.
- 952 Deevey ES, Nakai N, Stuiver M (1963) Fractionation of Sulfur and Carbon Isotopes in a  
953 Meromictic Lake. *Science*, **139**, 407-407.
- 954 Detmers J, Bruchert V, Habicht KS, Kuever J (2001) Diversity of Sulfur Isotope Fractionations  
955 by Sulfate-Reducing Prokaryotes. *Appl. Environ. Microbiol.*, **67**, 888-894.
- 956 Dickman M (1985) Seasonal succession and microlamina formation in a meromictic lake  
957 displaying varved sediments. *Sedimentology*, **32**, 109-118.
- 958 Dickman MD, Thode HG (1990) Sulfur bacteria and sulfur isotope fractionation in a meromictic  
959 lake near Toronto, Canada. In: *Facets of modern biogeochemistry* (eds Ihebhov V, Kempe  
960 S, Michaelis W, Spitzg A). Springer-Verlag, pp. 225-241.
- 961 Farquhar J, Bao H, Thiemens M (2000) Atmospheric Influence of Earth's Earliest Sulfur Cycle.  
962 *Science*, **289**, 756-758.
- 963 Farquhar J, Johnston DT, Wing BA (2007) Implications of conservation of mass effects on mass-  
964 dependent isotope fractionations: Influence of network structure on sulfur isotope phase  
965 space of dissimilatory sulfate reduction. *Geochimica et Cosmochimica Acta*, **71**, 5862-  
966 5875.
- 967 Farquhar J, Johnston DT, Wing BA, Habicht KS, Canfield DE, Airieau S, Thiemens MH (2003)  
968 Multiple sulphur isotopic interpretations of biosynthetic pathways: implications for  
969 biological signatures in the sulphur isotope record. *Geobiology*, **1**, 27-36.
- 970 Fike DA, Grotzinger JP, Pratt LM, Summons RE (2006) Oxidation of the Ediacaran Ocean.  
971 *Nature*, **444**, 744-747.
- 972 Fisher MM, Brenner M, Reddy KR (1992) A simple, inexpensive piston corer for collecting  
973 undisturbed sediment/water interface profiles. *Journal of Paleolimnology*, **7**, 157-161-  
974 161.
- 975 Fritz P, Basharmal GM, Drimmie RJ, Ibsen J, Qureshi RM (1989) Oxygen isotope exchange  
976 between sulphate and water during bacterial reduction of sulphate. *Chemical Geology*,  
977 **79**, 99-105.
- 978 Fry B (1986) Sources of Carbon and Sulfur Nutrition for Consumers in Three Meromictic Lakes  
979 of New York State. *Limnology and Oceanography*, **31**, 79-88.
- 980 Fry B, Cox J, Gest H, Hayes JM (1986) Discrimination between <sup>34</sup>S and <sup>32</sup>S during Bacterial  
981 Metabolism of Inorganic Sulfur Compounds. *Journal of Bacteriology*, **165**, 328-330.



- 982 Fry B, Gest H, Hayes JM (1984) Isotope effects associated with the anaerobic oxidation of  
983 sulfide by the purple photosynthetic bacterium, *Chromatium vinosum*. *FEMS*  
984 *Microbiology Letters*, **22**, 283-287.
- 985 Fry B, Gest H, Hayes JM (1988a)  $^{34}\text{S}/^{32}\text{S}$  fractionation in sulfur cycles catalyzed by anaerobic  
986 bacteria. *Appl. Environ. Microbiol.*, **54**, 250-256.
- 987 Fry B, Jannasch HW, Molyneaux SJ, Wirsen CO, Muramoto JA, King S (1991) Stable isotope  
988 studies of the carbon, nitrogen and sulfur cycles in the Black Sea and Cariaco Trench.  
989 *Deep Sea Research*, **38**, S1003-S1019.
- 990 Fry B, Ruf W, Gest H, Hayes JM (1988b) Sulfur Isotope Effects Associated with Oxidation of  
991 Sulfide by  $\text{O}_2$  in Aqueous Solution. *Chemical Geology*, **73**, 205-210.
- 992 Gibson JJ, Edwards TWD, Birks SJ, St Amour NA, Buhay WM, Mceachern P, Wolfe BB, Peters  
993 DL (2005) Progress in isotope tracer hydrology in Canada. *Hydrological Processes*, **19**,  
994 303-327.
- 995 Gibson JJ, Prepas EE, Mceachern P (2002) Quantitative comparison of lake throughflow,  
996 residency, and catchment runoff using stable isotopes: modelling and results from a  
997 regional survey of Boreal lakes. *Journal of Hydrology*, **262**, 128-144.
- 998 Habicht KS, Canfield DE, Rethmeier J (1998) Sulfur isotope fractionation during bacterial  
999 reduction and disproportionation of thiosulfate and sulfite. *Geochimica et Cosmochimica*  
1000 *Acta*, **62**, 2585-2595.
- 1001 Habicht KS, Gade M, Thamdrup B, Berg P, Canfield DE (2002) Calibration of Sulfate Levels in  
1002 the Archean Ocean. *Science*, **298**, 2372-2374.
- 1003 Hamilton T, Bovee R, Thiel V, Sattin S, Mohr W, Schaperdoth I, Vogl K, Gilhooly W, Lyons T,  
1004 Tomsho L (2014) Coupled reductive and oxidative sulfur cycling in the phototrophic  
1005 plate of a meromictic lake. *Geobiology*, **12**, 451-468.
- 1006 Harrison AG, Thode HG (1958) Mechanisms of the bacterial reduction of sulphate from isotope  
1007 fractionation studies. *Transactions of the Faraday Society*, **54**, 85-92.
- 1008 Heinrichs M, Wilson S, Walker I, Smol J, Mathewes R, Hall K (1997) Midge-and diatom-based  
1009 palaeosalinity reconstructions for Mahoney Lake, Okanagan Valley, British Columbia,  
1010 Canada. *International Journal of Salt Lake Research*, **6**, 249-267.
- 1011 Hoering TC, Kennedy JW (1957) The Exchange of Oxygen between Sulfuric Acid and Water I.  
1012 *Journal of the American Chemical Society*, **79**, 56-60.
- 1013 Holser WT, Kaplan IR, Sakai H, Zak I (1979) Isotope geochemistry of oxygen in the  
1014 sedimentary sulfate cycle. *Chemical Geology*, **25**, 1-17.
- 1015 Hurtgen MT, Arthur MA, Halverson GP (2005) Neoproterozoic sulfur isotopes, the evolution of  
1016 microbial sulfur species, and the burial efficiency of sulfide as sedimentary pyrite.  
1017 *Geology*, **33**, 41-44.
- 1018 Johnston DT, Farquhar J, Canfield DE (2007) Sulfur isotope insights into microbial sulfate  
1019 reduction: When microbes meet models. *Geochimica et Cosmochimica Acta*, **71**, 3929-  
1020 3947.
- 1021 Johnston DT, Wing BA, Farquhar J, Kaufman AJ, Strauss H, Lyons TW, Kah LC, Canfield DE  
1022 (2005) Active Microbial Sulfur Disproportionation in the Mesoproterozoic. *Science*, **310**,  
1023 1477-1479.
- 1024 Johnston DT, Wolfe-Simon F, Pearson A, Knoll AH (2009) Anoxygenic photosynthesis  
1025 modulated Proterozoic oxygen and sustained Earth's middle age. *Proceedings of the*  
1026 *National Academy of Sciences*, **106**, 16925-16929.

- 1027 Kaplan IR, Rittenberg SC (1964a) Microbiological Fractionation of Sulphur Isotopes. *Journal of*  
1028 *General Microbiology*, **34**, 195-212.
- 1029 Kaplan IR, Rittenberg SC (1964b) Microbiological Fractionation of Sulphur Isotopes.  
1030 *Microbiology*, **34**, 195-212.
- 1031 Kemp ALW, Thode HG (1968) The mechanism of the bacterial reduction of sulphate and of  
1032 sulphite from isotope fractionation studies. *Geochimica et Cosmochimica Acta*, **32**, 71-  
1033 91.
- 1034 Klepac-Ceraj V, Hayes CA, Gilhooly WP, Lyons TW, Kolter R, Pearson A (2012) Microbial  
1035 diversity under extreme euxinia: Mahoney Lake, Canada. *Geobiology*, **10**, 223-235.
- 1036 Knöller K, Vogt C, Richnow H-H, Weise S (2006) Sulfur and Oxygen Isotope Fractionation  
1037 during Benzene, Toluene, Ethyl Benzene, and Xylene Degradation by Sulfate-Reducing  
1038 Bacteria. *Environmental Science and Technology*, **40**, 3879-3885.
- 1039 Leavitt WD, Cummins R, Schmidt ML, Sim MS, Ono S, Bradley AS, Johnston DT (2014)  
1040 Multiple sulfur isotope signatures of sulfite and thiosulfate reduction by the model  
1041 dissimilatory sulfate-reducer, *Desulfovibrio alaskensis* str. G20. *Frontiers in*  
1042 *microbiology*, **5**.
- 1043 Leavitt WD, Halevy I, Bradley AS, Johnston DT (2013) Influence of sulfate reduction rates on  
1044 the Phanerozoic sulfur isotope record. *Proceedings of the National Academy of Sciences*,  
1045 **110**, 11244-11249.
- 1046 Lewis T (1984) Geothermal energy from Penticton Tertiary outlier, British Columbia: an initial  
1047 assessment. *Canadian Journal of Earth Sciences*, **21**, 181-188.
- 1048 Li X, Gilhooly Iii WP, Zerkle AL, Lyons TW, Farquhar J, Werne JP, Varela R, Scranton MI  
1049 (2010) Stable sulfur isotopes in the water column of the Cariaco Basin. *Geochimica et*  
1050 *Cosmochimica Acta*, **74**, 6764-6778.
- 1051 Lloyd RM (1968) Oxygen Isotope Behavior in the Sulfate-Water System. *Journal of*  
1052 *Geophysical Research*, **73**, 6099.
- 1053 Lowe DJ, Green JD, Northcote TG, Hall KJ (1997) Holocene Fluctuations of a Meromictic Lake  
1054 in Southern British Columbia. *Quaternary Research*, **48**, 100-113.
- 1055 Lyons TW (1997) Sulfur isotopic trends and pathways of iron sulfide formation in upper  
1056 Holocene sediments of the anoxic Black Sea. *Geochimica et Cosmochimica Acta*, **61**,  
1057 3367-3382.
- 1058 Lyons TW, Berner RA, Anderson RF (1993) Evidence for large pre-industrial perturbations of  
1059 the Black Sea chemocline. *Nature*, **365**, 538-540.
- 1060 Lyons TW, Kah LC, Gellatly AM (2004) The Precambrian sulphur isotope record of evolving  
1061 atmospheric oxygen. In: *The Precambrian Earth: Tempos and Events* (eds Eriksson PG,  
1062 Alterman W, Nelson DR, Mueller WU, Catuneanu O). Elsevier, Amsterdam, pp. 421-  
1063 440.
- 1064 Lyons TW, Severmann S (2006) A critical look at iron paleoredox proxies: New insights from  
1065 modern euxinic marine basins. *Geochimica et Cosmochimica Acta*, **70**, 5698-5722.
- 1066 Lyons TW, Werne JP, Hollander DJ, Murray RW (2003) Contrasting sulfur geochemistry and  
1067 Fe/Al and Mo/Al ratios across the last oxic-to-anoxic transition in the Cariaco Basin,  
1068 Venezuela. *Chemical Geology*, **195**, 131-157.
- 1069 Magaritz M, Taylor HP (1986) Oxygen 18/Oxygen 16 and D/H Studies of Plutonic Granitic and  
1070 Metamorphic Rocks Across the Cordilleran Batholiths of Southern British Columbia.  
1071 *Journal of Geophysical Research*, **91**, 2193-2217.

- 1072 Mandernack KW, Krouse HR, Skei JM (2003) A stable sulfur and oxygen isotopic investigation  
1073 of sulfur cycling in an anoxic marine basin, Framvaren Fjord, Norway. *Chemical*  
1074 *Geology*, **195**, 181-200.
- 1075 Mariotti A, Germon J, Hubert P, Kaiser P, Letolle R, Tardieux A, Tardieux P (1981)  
1076 Experimental determination of nitrogen kinetic isotope fractionation: Some principles;  
1077 illustration for the denitrification and nitrification processes. *Plant and Soil*, **62**, 413-430-  
1078 430.
- 1079 Meyer K, Macalady J, Fulton J, Kump L, Schaperdoth I, Freeman K (2011) Carotenoid  
1080 biomarkers as an imperfect reflection of the anoxygenic phototrophic community in  
1081 meromictic Fayetteville Green Lake. *Geobiology*, **9**, 321-329.
- 1082 Michel FA, Allen DM, Grant MB (2002) Hydrogeochemistry and geothermal characteristics of  
1083 the White Lake basin, South-central British Columbia, Canada. *Geothermics*, **31**, 169-  
1084 194.
- 1085 Mizutani Y (1972) Isotopic composition and underground temperature of the Otake geothermal  
1086 water Kyushu, Japan. *Geochemical Journal*, **6**, 67-73.
- 1087 Mizutani Y, Rafter TA (1969) Oxygen Isotopic Composition of Sulphates - Part 4. *New Zealand*  
1088 *Journal of Science*, **12**, 60-68.
- 1089 Mizutani Y, Rafter TA (1973) Isotopic behaviour of sulfate oxygen in the bacterial reduction of  
1090 sulfate. *Geochemical Journal*, **6**, 183-191.
- 1091 Neretin LN, Böttcher ME, Grinenko VA (2003) Sulfur isotope geochemistry of the Black Sea  
1092 water column. *Chemical Geology*, **200**, 59-69.
- 1093 Northcote T, Hall K (2010) Salinity regulation of zooplanktonic abundance and vertical  
1094 distribution in two saline meromictic lakes in south central British Columbia.  
1095 *Hydrobiologia*, **638**, 121-136.
- 1096 Northcote TG, Hall KJ (1983) Limnological contrasts and anomalies in two adjacent saline  
1097 lakes. *Hydrobiologia*, **105**, 179-194.
- 1098 Northcote TG, Hall KJ (1990) Vernal microstratification patterns in a meromictic saline lake:  
1099 their causes and biological significance. *Hydrobiologia*, **197**, 105-114-114.
- 1100 Northcote TG, Hall KJ (2000) Short-term (decadal, annual, seasonal) changes in the limnology  
1101 of a saline uni-/bimeromictic lake: causes and consequences. *Verhandlungen*  
1102 *Internationale Vereinigen für theoretische und angewandte Limnologie* **27**, 2652-2659.
- 1103 Northcote TG, Halsey TG (1969) Seasonal changes in the limnology of some meromictic lakes  
1104 in southern British Columbia. *Journal Fisheries Research Board of Canada*, **26**, 1763-  
1105 1787.
- 1106 Ohmoto H, Lasaga AC (1982) Kinetics of reactions between aqueous sulfates and sulfides in  
1107 hydrothermal systems. *Geochimica et Cosmochimica Acta*, **46**, 1727-1745.
- 1108 Overmann J (1997) Mahoney Lake: A case study of the ecological significance of phototrophic  
1109 sulfur bacteria. In: *Advances in Microbial Ecology* (ed Jones JG). Plenum Press, New  
1110 York.
- 1111 Overmann J, Beatty JT, Hall KJ, Pfennig N, Northcote TG (1991) Characterization of a dense,  
1112 purple sulfur bacterial layer in a meromictic salt lake. *Limnology and Oceanography*, **36**,  
1113 846-859.
- 1114 Overmann J, Beatty JT, Krouse HR, Hall KJ (1996) The sulfur cycle in the chemocline of a  
1115 meromictic salt lake. *Limnology and Oceanography*, **4**, 147-156.
- 1116 Overmann J, Pfennig N (1992) Bouyancy regulation and aggregate formation in *Amoebobacter*  
1117 *purpureus* from Mahoney Lake. *FEMS Microbiology Letters*, **101**, 67-79.

- 1118 Overmann J, Sandmann G, Hall KJ, Northcote TG (1993) Fossil carotenoids and paleolimnology  
1119 of meromictic Mahoney Lake, British Columbia, Canada. *Aquatic Sciences - Research*  
1120 *Across Boundaries*, **55**, 31-39.
- 1121 Overmann J, Thomas Beatty J, Hall KJ (1994) Photosynthetic activity and population dynamics  
1122 of *Amoebobacter purpureus* in a meromictic saline lake. *FEMS Microbiology Ecology*,  
1123 **15**, 309-319.
- 1124 Raiswell R, Buckley F, Berner RA, Anderson TF (1988) Degree of pyritization of iron as a  
1125 paleoenvironmental indicator of bottom-water oxygenation. *Journal of Sedimentary*  
1126 *Research*, **58**, 812-819.
- 1127 Raiswell R, Canfield DE, Berner RA (1994) A comparison of iron extraction methods for the  
1128 determination of degree of pyritisation and the recognition of iron-limited pyrite  
1129 formation. *Chemical Geology*, **111**, 101-110.
- 1130 Rees CE (1973) A steady-state model for sulphur isotope fractionation in bacterial reduction  
1131 processes. *Geochimica et Cosmochimica Acta*, **37**, 1141-1162.
- 1132 Rees CE (1978) The sulphur isotopic composition of ocean water sulphate. *Geochimica et*  
1133 *Cosmochimica Acta*, **42**, 377-381.
- 1134 Reinhard CT, Planavsky NJ, Robbins LJ, Partin CA, Gill BC, Lalonde SV, Bekker A, Konhauser  
1135 KO, Lyons TW (2013) Proterozoic ocean redox and biogeochemical stasis. *Proceedings*  
1136 *of the National Academy of Sciences*, **110**, 5357-5362.
- 1137 Riedinger N, Brunner B, Formolo MJ, Solomon E, Kasten S, Strasser M, Ferdelman TG (2010)  
1138 Oxidative sulfur cycling in the deep biosphere of the Nankai Trough, Japan. *Geology*, **38**,  
1139 851-854.
- 1140 Rudnicki MD, Elderfield H, Spiro B (2001) Fractionation of sulfur isotopes during bacterial  
1141 sulfate reduction in deep ocean sediments at elevated temperatures. *Geochimica et*  
1142 *Cosmochimica Acta*, **65**, 777-789.
- 1143 Sheu D-D, Shakur A, Pigott JD, Wiesenburg DA, Brooks JM, Krouse HR (1988) Sulfur and  
1144 oxygen isotopic compositions of dissolved sulfate in the Orca Basin: Implications for  
1145 origin of the high-salinity brine and oxidation of sulfides at the brine-seawater interface.  
1146 *Marine Geology*, **78**, 303-310.
- 1147 Sim MS, Bosak T, Ono S (2011) Large Sulfur Isotope Fractionation Does Not Require  
1148 Disproportionation. *Science*, **333**, 74-77.
- 1149 Sørensen KB, Canfield DE (2004) Annual fluctuations in sulfur isotope fractionation in the water  
1150 column of a euxinic marine basin. *Geochimica et Cosmochimica Acta*, **68**, 503-515.
- 1151 Stookey LL (1970) Ferrozine---a new spectrophotometric reagent for iron. *Analytical Chemistry*,  
1152 **42**, 779-781.
- 1153 Sweeney RE, Kaplan IR (1980) Stable isotope composition of dissolved sulfate and hydrogen  
1154 sulfide in the Black Sea. *Marine Chemistry*, **9**, 145-152.
- 1155 Taylor BE, Wheeler MC (1984) Isotope composition of sulphate in acid mine drainage as  
1156 measure of bacterial oxidation. *Nature*, **308**, 538-541.
- 1157 Thamdrup B, Finster K, Hansen JW, Bak F (1993) Bacterial Disproportionation of Elemental  
1158 Sulfur Coupled to Chemical Reduction of Iron or Manganese. *Applied and*  
1159 *Environmental Microbiology*, **59**, 101-108.
- 1160 Turchyn AV, Brüchert V, Lyons TW, Engel GS, Balci N, Schrag DP, Brunner B (2010) Kinetic  
1161 oxygen isotope effects during dissimilatory sulfate reduction: a combined theoretical and  
1162 experimental approach. *Geochimica et Cosmochimica Acta*, **74**, 2011-2024.

- 1163 Turchyn AV, Schrag DP (2006) Cenozoic evolution of the sulfur cycle: Insight from oxygen  
1164 isotopes in marine sulfate. *Earth and Planetary Science Letters*, **241**, 763-779.
- 1165 Turchyn AV, Schrag DP, Coccioni R, Montanari A (2009) Stable isotope analysis of the  
1166 Cretaceous sulfur cycle. *Earth and Planetary Science Letters*, **285**, 115-123.
- 1167 Van Everdingen RO, Krouse HR (1985) Isotope composition of sulphates generated by bacterial  
1168 and abiological oxidation. *Nature*, **315**, 395-396.
- 1169 Ward PRB, Cousins EA, Hall KJ, Northcote TG, Murphy TP (1989) Mixing by Wind and  
1170 Penetrative Convection in Small Lakes. In: *International Association for Hydraulic  
1171 Research, 23rd. Congress*, Ottawa, Canada, pp. D-331-D-338.
- 1172 Ward PRB, Hall KJ, Northcote TG, Cheung W, Murphy T (1990) Autumnal mixing in Mahoney  
1173 Lake, British Columbia. *Hydrobiologia*, **197**, 129-138-138.
- 1174 Wehrmann LM, Templer SP, Brunner B, Bernasconi SM, Maignien L, Ferdelman TG (2011)  
1175 The imprint of methane seepage on the geochemical record and early diagenetic  
1176 processes in cold-water coral mounds on Pen Duick Escarpment, Gulf of Cadiz. *Marine  
1177 Geology*, **282**, 118-137.
- 1178 West AG, Patrickson SJ, Ehleringer JR (2006) Water extraction times for plant and soil materials  
1179 used in stable isotope analysis. *Rapid Communications in Mass Spectrometry*, **20**, 1317-  
1180 1321.
- 1181 Wortmann UG, Bernasconi SM, Bottcher ME (2001) Hypersulfidic deep biosphere indicates  
1182 extreme sulfur isotope fractionation during single-step microbial sulfate reduction.  
1183 *Geology*, **29**, 647-650.
- 1184 Wortmann UG, Chernyavsky B, Bernasconi SM, Brunner B, Böttcher ME, Swart PK (2007)  
1185 Oxygen isotope biogeochemistry of pore water sulfate in the deep biosphere: Dominance  
1186 of isotope exchange reactions with ambient water during microbial sulfate reduction  
1187 (ODP Site 1130). *Geochimica et Cosmochimica Acta*, **71**, 4221-4232.
- 1188 Zak I, Saki H, Kaplan IR (1980) Factors Controlling the  $^{18}\text{O}/^{16}\text{O}$  and  $^{34}\text{S}/^{32}\text{S}$  Isotope Ratios of  
1189 Ocean Sulfates, Evaporites and Interstitial Sulfates from Modern Deep Sea Sediments.  
1190 In: *Isotope Marine Chemistry* (eds Goldberg ED, Horibe Y, Saruhashi K). Geochemistry  
1191 Research Association, Tokyo, pp. 339-373.
- 1192 Zeebe RE (2010) A new value for the stable oxygen isotope fractionation between dissolved  
1193 sulfate ion and water. *Geochimica et Cosmochimica Acta*, **74**, 818-828.
- 1194 Zerkle AL, Farquhar J, Johnston DT, Cox RP, Canfield DE (2009) Fractionation of multiple  
1195 sulfur isotopes during phototrophic oxidation of sulfide and elemental sulfur by a green  
1196 sulfur bacterium. *Geochimica et Cosmochimica Acta*, **73**, 291-306.
- 1197 Zerkle AL, Kamyshny Jr A, Kump LR, Farquhar J, Oduro H, Arthur MA (2010) Sulfur cycling  
1198 in a stratified euxinic lake with moderately high sulfate: Constraints from quadruple S  
1199 isotopes. *Geochimica et Cosmochimica Acta*, **74**, 4953-4970.
- 1200 Zhang J-Z, Millero FJ (1994) Kinetics of Oxidation of Hydrogen Sulfide in Natural Waters. In:  
1201 *Environmental Geochemistry of Sulfide Oxidation* (eds Alpers CN, Blowes DW).  
1202 American Chemical Society, Washington DC, pp. 393-409.
- 1203 Zopf J, Ferdelman TG, Jörgensen BB, Teske A, Thamdrup B (2001) Influence of water column  
1204 dynamics on sulfide oxidation and other major biogeochemical processes in the  
1205 chemocline of Mariager Fjord (Denmark). *Marine Chemistry*, **74**, 29-51.
- 1206

1208 Figure 1. Mahoney Lake and Green Lake are located within the White Lake Basin, British  
 1209 Columbia (modified after Northcote and Hall, 1983; Michel et al, 2002). Cores 2 and 3 were  
 1210 collected from the center of Mahoney Lake and Core 9 was taken from the oxic margin. Surface  
 1211 water  $\delta^{34}\text{S}_{\text{SO}_4}$ ,  $\delta^{18}\text{O}_{\text{SO}_4}$ , and sulfate concentrations are shown for Mahoney Lake, Green Lake,  
 1212 Sleeping Lake, and the upland pond (ML pond), as well as the  $\delta^{34}\text{S}$  of chromium reducible sulfur  
 1213 extracted from a greenstone sample collected from the eastern side of the catchment. Bedrock  
 1214 geology transitions from meta-volcanics west of the fault-line to cherts and greenstones east of  
 1215 the fault. Geologic descriptions and interpretations are from Church (2002) and Northcote and  
 1216 Hall (1983).

1217  
 1218  
 1219 Figure 2. Oxygen and hydrogen isotope data for meteoric water and surface waters in the White  
 1220 Lake Basin. Results from the current study include samples from the Mahoney Lake  
 1221 mixolimnion (ML 08 oxic) and monimolimnion (ML 08 anoxic), the upland pond (ML pond 08),  
 1222 and Sleeping Lake (SL 08). All remaining water data are from Michel et al., (2002). The Local  
 1223 Meteoric Water Line (LMWL) is shown for Penticton precipitation data (squares) in comparison  
 1224 to the Global Meteoric Water Line (GMWL;  $\delta\text{D} = 8\delta^{18}\text{O} + 10$ ). Data for deep wells (open  
 1225 diamonds; 76 to 549 m deep), shallow wells drilled in overburden (filled diamonds), springs  
 1226 (triangles), and surface waters (circles) all plot along a local evaporation line (LEL) with a slope  
 1227 of 4.7 ( $R^2 = 0.99$ ). The inset shows LEL relative to the isotopic composition of Vienna Standard  
 1228 Mean Oceanwater (VSMOW) and Okanagan granitic batholiths (Magaritz and Taylor, 1986).

1229  
 1230  
 1231 Figure 3. Water column profiles of temperature, specific conductivity (SpC), pH, dissolved  
 1232 oxygen (DO), dissolved sulfide ( $\text{H}_2\text{S}$ ), light intensity, and turbidity for (A) Mahoney and Green  
 1233 Lake in September 2006, and (B) Mahoney Lake in July 2008. Extinction coefficients ( $k$ ) were  
 1234 calculated for light attenuation above ( $k = 0.400$ ) and below the chemocline ( $k = 3.347$ ) in  
 1235 Mahoney Lake, July 2008.

1236  
 1237  
 1238 Figure 4. Mahoney Lake water column profiles of chloride and sulfate concentrations,  $\text{SO}_4/\text{Cl}$   
 1239 (molar),  $\delta^{34}\text{S}_{\text{H}_2\text{S}}$ ,  $\delta^{34}\text{S}_{\text{SO}_4}$ , and  $\delta^{18}\text{O}_{\text{SO}_4}$  for samples collected in September 2006 (filled symbols)  
 1240 and July 2008 (open symbols). Vertical shaded regions are the mean plus standard deviations for  
 1241 concentrations ( $[\text{Cl}] = 57.7 \pm 1.7 \text{ mM}$ ;  $[\text{SO}_4] = 341 \pm 20.1 \text{ mM}$ ) or molar ratios ( $\text{SO}_4/\text{Cl} = 5.9 \pm$   
 1242  $0.2$ ) within the upper 5 m of the (oxygenated) water column.

1243  
 1244  
 1245 Figure 5. Mahoney Lake (A) solid phase sulfur concentrations, DOS, and (B) solid phase and  
 1246 pore water isotope data for sediments collected below the chemocline (Core 2 and 3) and below  
 1247 oxygenated bottom water (Core 9). Vertical shaded regions (B) indicate the average stable  
 1248 isotope value ( $\pm$  standard deviation) of water column sulfate and sulfide.

1249  
 1250  
 1251 Figure 6. Mahoney Lake sulfur isotope fractionation ( $\Delta^{34}\text{S}_{\text{SO}_4\text{-H}_2\text{S}} = \delta^{34}\text{S}_{\text{SO}_4} - \delta^{34}\text{S}_{\text{H}_2\text{S}}$ ) within the  
 1252 water column (round symbols) and averaged pore water values from Cores 2 and 3 (open  
 1253 diamonds) and Core 9 (filled diamonds) plotted against depth. Error bars represent standard

1254 deviation for fractionations. Cores 2 and 3 were collected below the chemocline and Core 9 was  
1255 collected below oxygenated bottom waters.

1256

1257

1258 Figure 7. Sulfate sulfur and oxygen isotope cross-plots of Mahoney Lake water column sulfate  
1259 collected in September 2006 (filled symbols) and July 2008 (open symbols). The data are  
1260 bounded by model arrays (A) that define the expected trajectories of rapid sulfate reduction,  
1261 Trend A, and slow rates of sulfate reduction, Trend B, based on the initial isotopic compositions  
1262 for Mahoney Lake sulfate ( $\delta^{34}\text{S}_{\text{SO}_4} = 21.5\text{‰}$  and  $\delta^{18}\text{O}_{\text{SO}_4} = 16.5\text{‰}$ ; filled square) and water  
1263 ( $\delta^{18}\text{O}_{\text{water}} = -0.3\text{‰}$ ). The data collected in the fall (B) have a higher slope than the those collected  
1264 in the summer (C).

1265

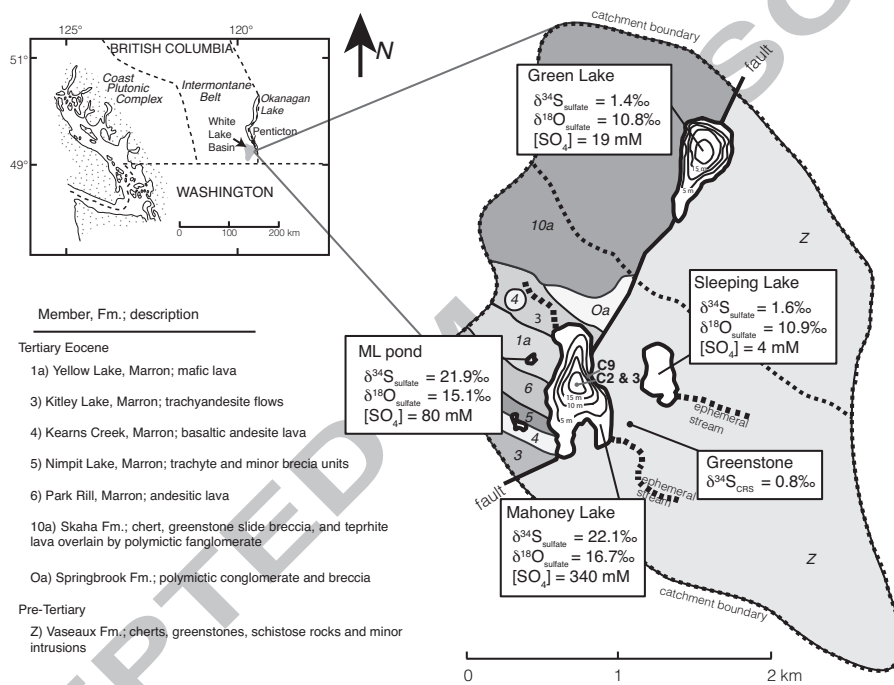
1266

1267 Figure 8. Mixing plots ( $\delta$  vs.  $1/\text{concentration}$ ) of sulfate (A) sulfur isotope and (B) oxygen  
1268 isotope values relative to sulfate concentration for Mahoney Lake water column (round symbols)  
1269 and power waters (diamonds) collected from anoxic (open symbols) or oxic (closed symbols)  
1270 bottom waters.

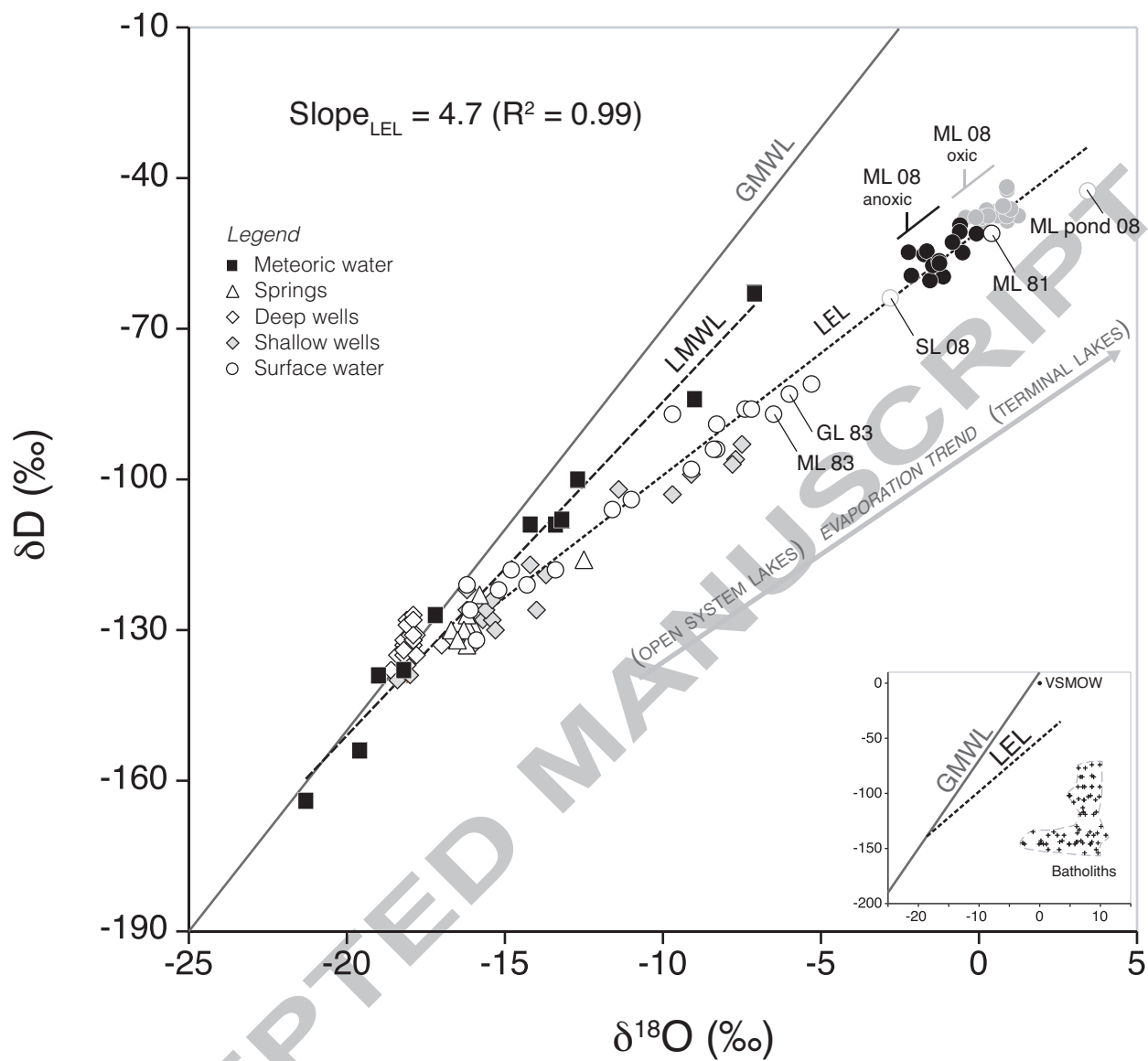
1271

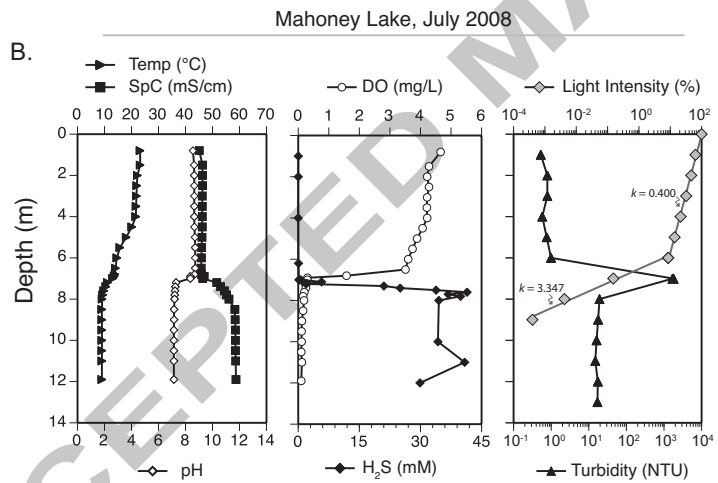
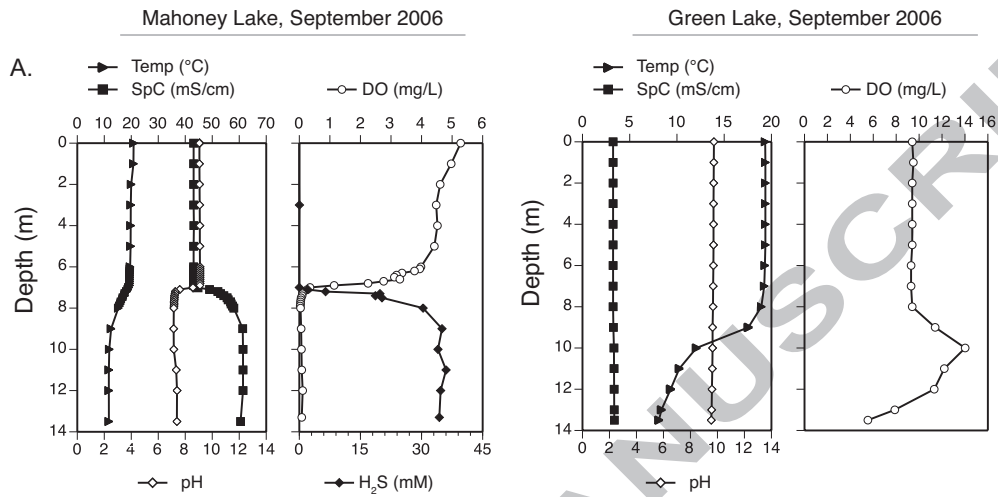
1272

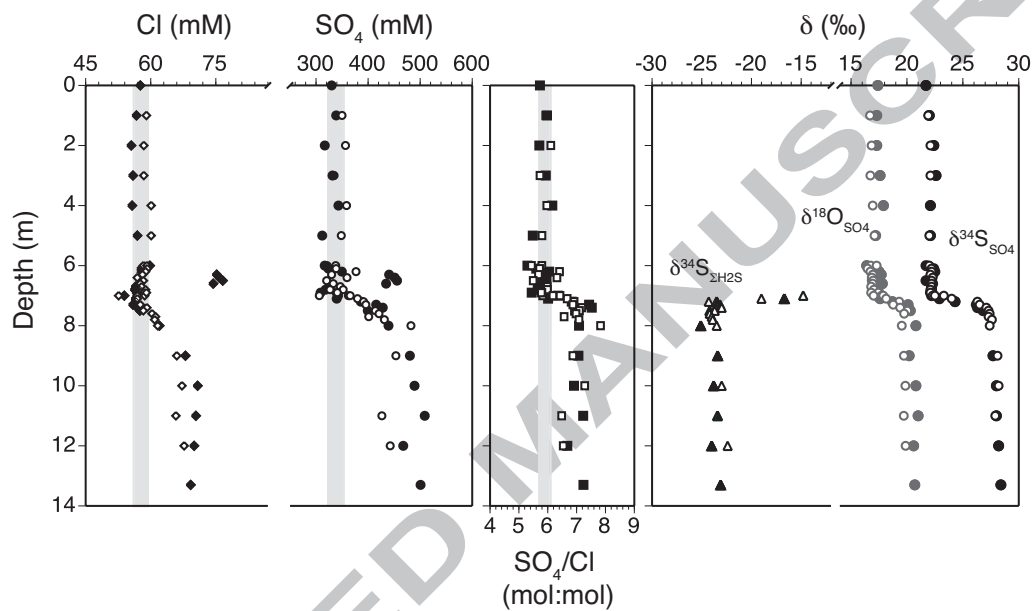
1273

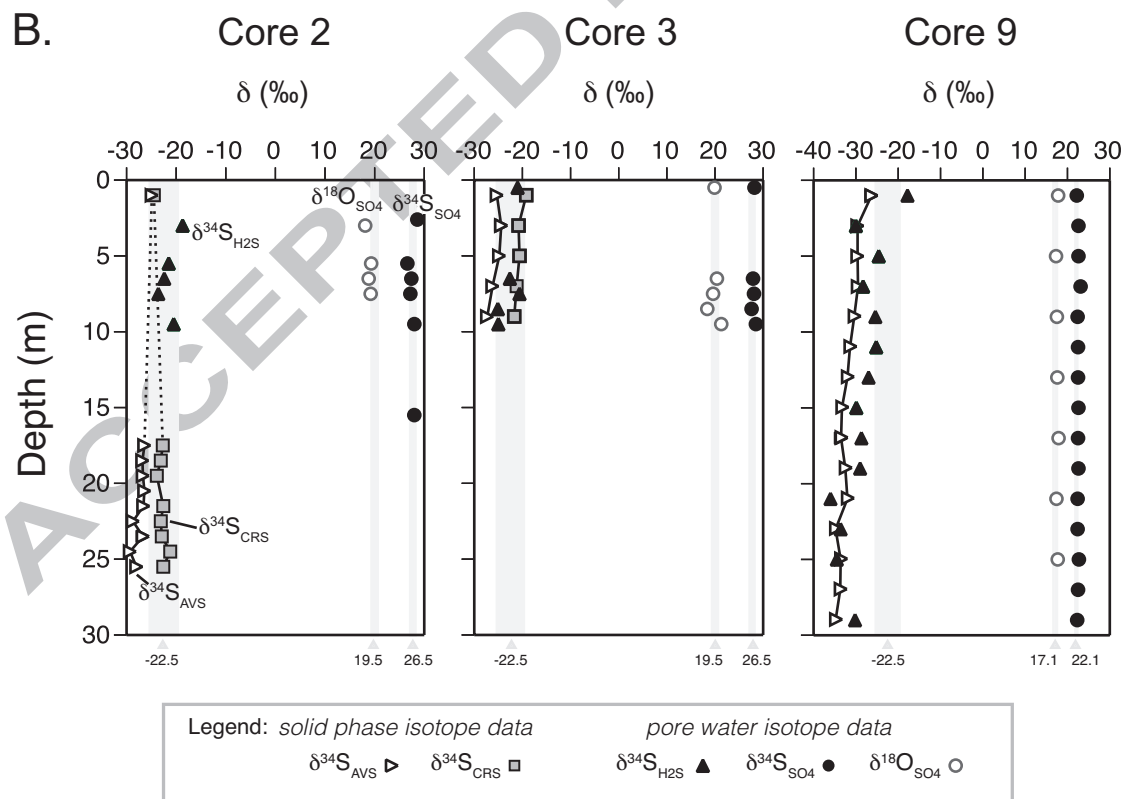
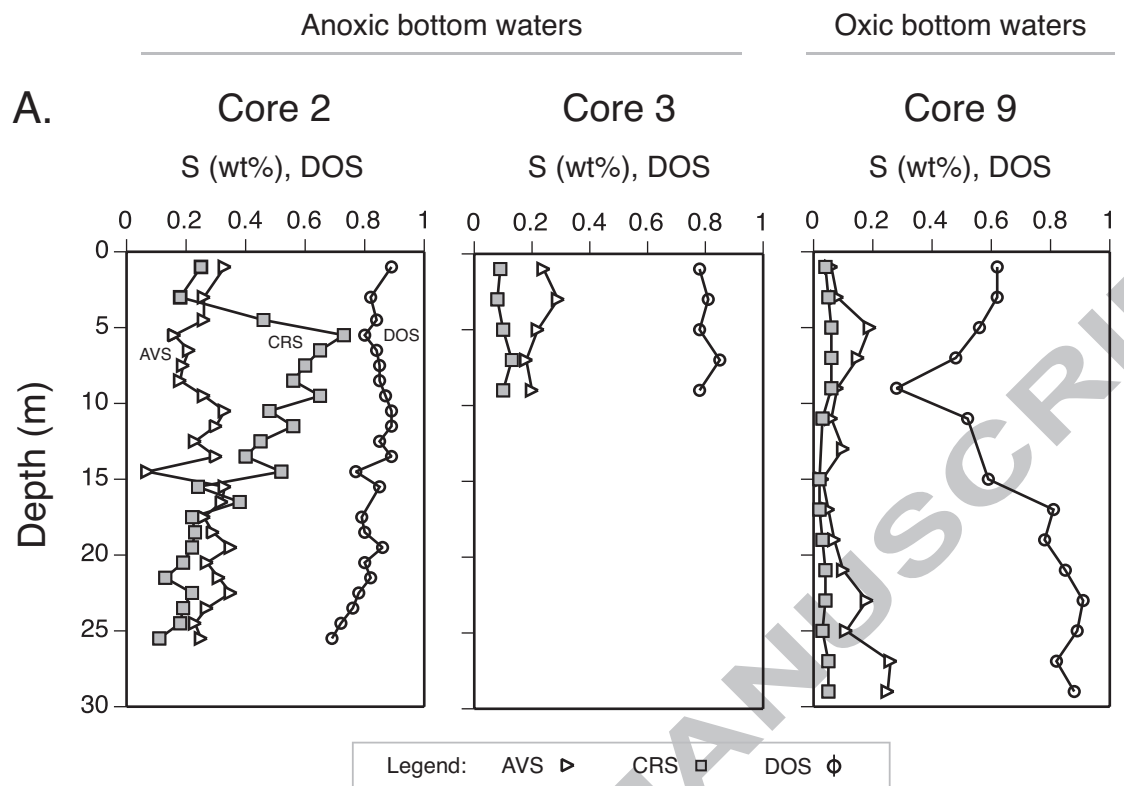


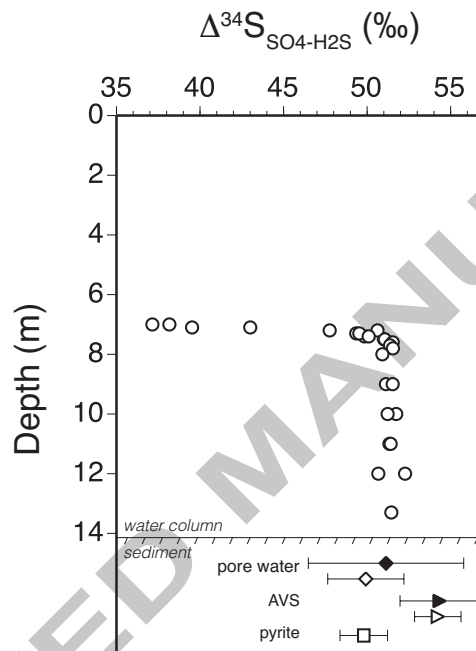


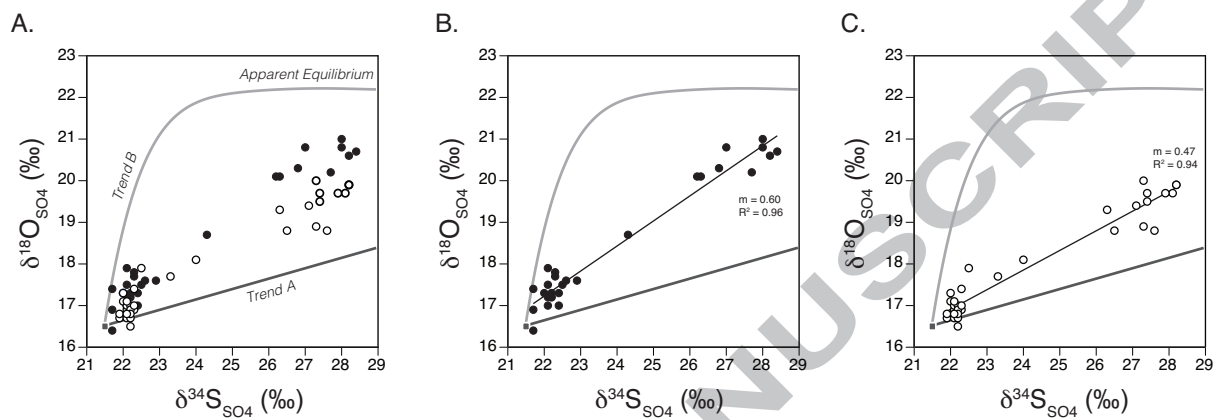
1276  
1277



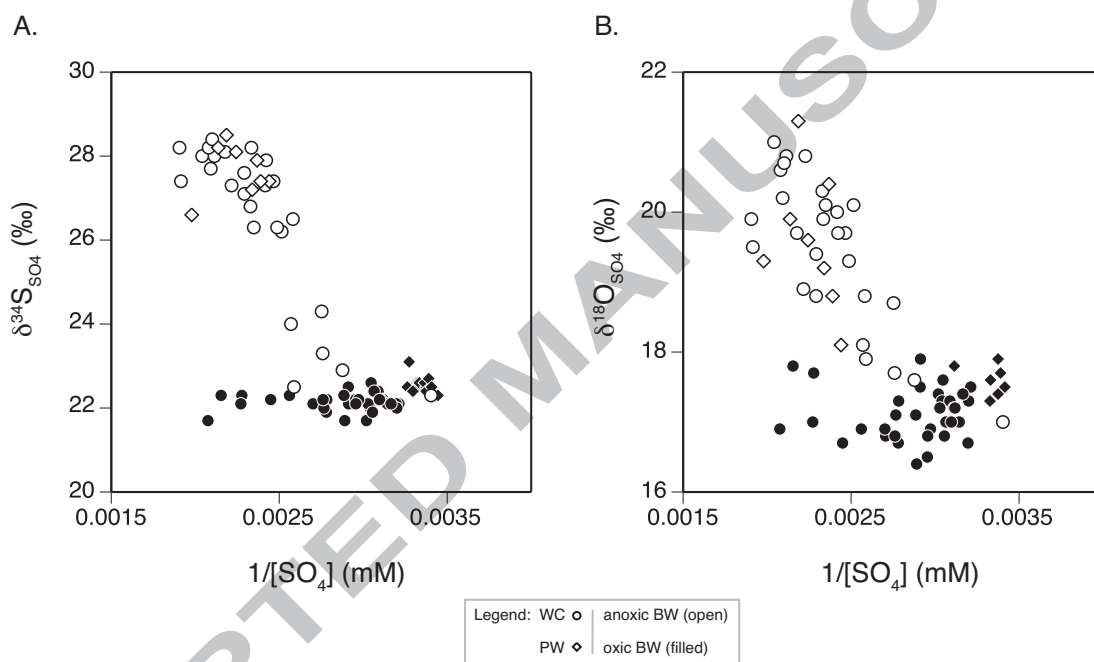








1286  
1287



1289 Table 1. Water column concentration and isotope data.

Lake	Dep th (m)	$\Sigma\text{H}_2\text{S}$ (m M)	$\text{SO}_4$ (m M)	Cl (m M)	$\delta^{18}\text{O}$ $\text{SO}_4$ (‰)	$\delta^{34}\text{S}$ $\text{SO}_4$ (‰)	$\delta^{34}\text{S}$ $\text{H}_2\text{S}$ (‰)	$\Delta^{34}\text{S}_{\text{SO}_4}$ $-\text{H}_2\text{S}$ (‰)	$\delta^{34}\text{S}_{\text{Elem}}$ S (‰)	$\delta^{18}\text{O}$ $\text{H}_2\text{O}$ (‰)	$\delta^2\text{H}_\text{H}$ 2O (‰)
<i>September 2006</i>											
Green Lake	0	-	24. 94	1.4	11.6	5.2	-	-	-	-	-
	1	-	19. 90	0.4	10.5	1.2	-	-	-	-	-
	2	-	20. 74	0.2	10.2	1.2	-	-	-	-	-
	3	-	18. 52	0.4	10.9	1.2	-	-	-	-	-
	4	-	20. 04	0.4	10.6	1.0	-	-	-	-	-
	5	-	19. 33	1	10.7	0.5	-	-	-	-	-
	6	-	20. 22	-	10.5	1.1	-	-	-	-	-
	7	-	20. 29	2.3	10.5	1.1	-	-	-	-	-
	9	-	20. 09	1.3	11.2	1.1	-	-	-	-	-
	10	-	20. 90	0.7	11.0	1.2	-	-	-	-	-
	11	-	21. 30	0.7	-	1.0	-	-	-	-	-
	12	-	21. 71	-	10.9	1.1	-	-	-	-	-
	13	-	20. 13	-	11.1	0.7	-	-	-	-	-
Mahoney Lake	0	-	331 .2	57. 6	17.4	21.7	-	-	-	-	-
	1	-	328 .8	56. 7	17.3	22.0	-	-	-	-	-
	2	-	323 .8	55. 5	17.3	22.4	-	-	-	-	-
	3	0.0 29	328 .2	55. 9	17.6	22.6	-	-	-	-	-
	4	-	343 .3	55. 7	17.9	22.1	-	-	-	-	-
	5	-	330 .2	56. 9	17.2	22.1	-	-	-	-	-



Lake	Dep th (m)	$\Sigma H_2S$			$\delta^{18}O$	$\delta^{34}S$	$\delta^{34}S$	$\Delta^{34}S_{SO_4}$	$\delta^{34}S_{Elem}$	$\delta^{18}O$	$\delta^2H_H$
		S (m M)	SO <sub>4</sub> (m M)	Cl (m M)	SO <sub>4</sub> (‰)	SO <sub>4</sub> (‰)	H <sub>2</sub> S (‰)	-H <sub>2</sub> S (‰)	S (‰)	H <sub>2</sub> O (‰)	2O (‰)
			346	59.							
	6	-	.0	8	16.4	21.7	-	-	-	-	-
			326	57.							
	6.1	-	.3	8	17.0	22.4	-	-	-	-	-
			343	57.							
	6.2	-	.5	8	17.5	22.5	-	-	-	-	-
			439	75.							
	6.3	-	.1	2	17.7	22.3	-	-	-	-	-
			440	75.							
	6.4	-	.2	8	17.0	22.1	-	-	-	-	-
			481	76.							
	6.5	-	.8	6	16.9	21.7	-	-	-	-	-
			464	74.							
	6.6	-	.2	4	17.8	22.3	-	-	-	-	-
			321	56.							
	6.7	-	.4	5	17.2	22.2	-	-	-	-	-
			320	56.							
	6.8	-	.7	3	17.2	22.2	-	-	-	-	-
			311	56.							
	6.9	-	.3	7	17.5	22.1	-	-	-	-	-
			359	53.							
	7	-	.3	9	17.3	22.2	-	-	-	-	-
			2.0	347	56.						
	7.1	8	.6	5	17.6	22.9	-16.7	39.5	-	-	-
			6.4	363	56.						
	7.2	5	.3	5	18.7	24.3	-23.5	47.8	-22.7	-	-
			19.	397	55.						
	7.3	79	.7	9	20.1	26.2	-23.2	49.3	-	-	-
			18.	425	56.						
	7.4	68	.8	9	20.1	26.3	-23.6	49.8	-	-	-
			20.	429	57.						
	7.5	29	.4	5	20.3	26.8	-24.2	51.0	-	-	-
			30.	448	62.						
	8	38	.9	0	20.8	27.0	-25.1	52.1	-	-	-
			35.	477	68.						
	9	02	.9	0	20.2	27.7	-23.4	51.1	-	-	-
			34.	473	70.						
	10	03	.0	8	20.8	28.0	-23.8	51.7	-	-	-
			36.	489	70.						
	11	02	.9	4	21.0	28.0	-23.4	51.3	-	-	-
			34.	480	70.						
	12	68	.8	0	20.6	28.2	-24.0	52.3	-	-	-

Lake	Depth (m)	$\Sigma\text{H}_2\text{S}$ (mM)	$\text{SO}_4$ (mM)	$\text{Cl}$ (mM)	$\delta^{18}\text{O}_{\text{SO}_4}$ (‰)	$\delta^{34}\text{S}_{\text{SO}_4}$ (‰)	$\delta^{34}\text{S}_{\text{H}_2\text{S}}$ (‰)	$\Delta^{34}\text{S}_{\text{SO}_4-\text{H}_2\text{S}}$ (‰)	$\delta^{34}\text{S}_{\text{Elem S}}$ (‰)	$\delta^{18}\text{O}_{\text{H}_2\text{O}}$ (‰)	$\delta^2\text{H}_{\text{H}_2\text{O}}$ (‰)
	13.3	34.36	475.9	69.2	20.7	28.4	-23.1	51.4	-	-	-
<i>July 2008</i>											
Mahoney Lake	1	0.031	359.6	59.0	16.7	21.9	-	-	-	0.89	48.51
	2	0.012	369.6	58.4	16.8	22.1	-	-	-	0.89	47.37
	3	-	312.9	58.4	16.7	22.1	-	-	-	1.24	47.50
	4	0.003	370.2	60.1	16.9	22.1	-	-	-	0.89	42.37
	5	-	361.5	60.1	17.1	22.0	-	-	-	0.76	46.86
	6	-	327.3	58.3	16.8	21.9	-	-	-	0.88	41.78
	6.0	-	312.5	59.1	17.3	22.0	-	-	-	0.60	47.50
	6.1	-	338.5	59.2	16.5	22.2	-	-	-	0.88	47.52
	6.2	0.062	408.3	58.8	16.7	22.2	-	-	-	0.79	45.67
	6.3	-	318.1	58.1	17.0	22.1	-	-	-	1.00	46.15
	6.4	-	390.5	56.9	16.9	22.3	-	-	-	0.24	46.38
	6.5	-	322.9	58.3	17.0	22.2	-	-	-	0.10	47.80
	6.6	-	336.4	57.6	16.9	22.2	-	-	-	0.76	45.54

Lake	Depth (m)	$\Sigma\text{H}_2\text{S}$			$\delta^{18}\text{O}$	$\delta^{34}\text{S}$	$\delta^{34}\text{S}$	$\Delta^{34}\text{S}_{\text{SO}_4}$	$\delta^{34}\text{S}_{\text{Elem}}$	$\delta^{18}\text{O}$	$\delta^2\text{H}_\text{H}$
		S (m M)	$\text{SO}_4$ (m M)	Cl (m M)	$\text{SO}_4$ (‰)	$\text{SO}_4$ (‰)	$\text{H}_2\text{S}$ (‰)	$-\text{H}_2\text{S}$ (‰)	S (‰)	$\text{H}_2\text{O}$ (‰)	$2\text{O}$ (‰)
			362	57.							47.8
	6.7	-	.2	9	16.8	22.2	-	-	-	-0.42	7
			352	58.							47.5
	6.8	-	.2	8	-	-	-	-	-	0.29	2
			315	57.							46.6
	6.8	-	.9	4	17.1	22.1	-	-	-	0.53	8
			346	58.							-
	6.9	-	.6	4	17.4	22.3	-	-	-	-	-
			338	59.							48.8
	6.9	-	.3	0	16.8	22.1	-	-	-	0.11	9
		0.1	386	56.							-
	7.0	9	.4	9	17.9	22.5	-	-	-	-	-
			293	52.							54.8
	7.0	0.2	.8	6	17.0	22.3	-14.8	37.1	-20.0, - 20.8	-0.52	4
			362	58.							47.8
	7.0	0.6	.5	6	17.7	23.3	-14.8	38.2	-	-0.10	2
			389	56.							49.3
	7.1	5.7	.1	9	18.1	24.0	-19.0	43.0	-	-0.60	6
			402	56.							50.6
	7.2	1.9	.0	6	19.3	26.3	-24.3	50.6	-	-0.61	9
			387	57.							52.7
	7.3	21.	.4	6	18.8	26.5	-23.1	49.5	-	-0.84	6
			436	59.							51.0
	7.4	25.	.2	1	19.4	27.1	-23.0	50.1	-	-0.08	6
			413	58.							54.5
	7.5	33.	.8	3	20.0	27.3	-23.7	51.1	-	-1.65	5
			405	60.							57.4
	7.6	41.	.5	3	19.7	27.4	-24.2	51.5	-	-1.46	0
			451	61.							-
	7.7	36.	.2	1	18.9	27.3	-24.0	51.4	-	-1.26	56.4

Lake	Depth (m)	$\Sigma H_2S$			$\delta^{18}O$	$\delta^{34}S$	$\delta^{34}S$	$\Delta^{34}S_{SO_4}$	$\delta^{34}S_{Elem}$	$\delta^{18}O$	$\delta^2H_H$
		S (mM)	SO <sub>4</sub> (mM)	Cl (mM)	SO <sub>4</sub> (‰)	SO <sub>4</sub> (‰)	H <sub>2</sub> S (‰)	-H <sub>2</sub> S (‰)	S (‰)	H <sub>2</sub> O (‰)	20 (‰)
											7
											-
	7.8	39.85	436.4	60.9	18.8	27.6	-23.9	51.5	-	-1.25	56.97
											-
	8	34.51	522.2	61.6	19.5	27.4	-23.5	50.9	-	-1.13	59.63
											-
	9	31.42	459.3	66.0	19.7	28.1	-23.4	51.5	-	-2.23	54.77
											-
	10	34.29	524.6	67.2	19.9	28.2	-23.0	51.2	-	-1.74	55.20
											-
	11	40.85	412.8	65.8	19.7	27.9	-23.5	51.4	-	-2.14	59.40
											-
	12	29.89	428.4	67.7	19.9	28.2	-22.4	50.7	-	-1.55	60.40
											-
ML Pond	0	-	79.9	22.3	15.1	21.9	-	-	-	3.44	42.55
											-
Sleeping Lake	0	-	4.0	14.8	10.9	1.6	-	-	-	-2.81	63.86

Table 2. Concentration and isotope data for solid phase sulfur species extracted from Mahoney Lake sediment cores recovered below the chemocline (Anoxic cores) and above the interface (Oxic core).

Core	Depth (cm)	AVS-S (wt. %)	Pyrite-S (wt. %)	Fe <sub>HCl</sub> (ppm)	DOS	$\delta^{34}\text{S}_{\text{AVS}}$ (‰)	$\delta^{34}\text{S}_{\text{Pyrite}}$ (‰)	$\delta^{34}\text{S}_{\text{Organic}}$ (‰)	$\Delta^{34}\text{S}_{\text{SO}_4\text{-AVS}}$ <sup>*</sup> (‰)	$\Delta^{34}\text{S}_{\text{SO}_4\text{-Pyrite}}$ <sup>*</sup> (‰)
<i>Anoxic cores</i>										
Core 2	1	0.33	0.25	967.1	0.89	-24.9	-24.5	-	52.6	52.2
	3	0.26	0.18	1357.4	0.82	-	-	-19.3	-	-
	4.5	0.26	0.46	1571.9	0.84	-	-	-20.9	-	-
	5.5	0.16	0.73	2376.4	0.80	-	-	-	-	-
	6.5	0.21	0.65	1750.9	0.84	-	-	-	-	-
	7.5	0.19	0.60	1510.1	0.85	-	-	-	-	-
	8.5	0.18	0.56	1409.4	0.85	-	-	-	-	-
	9.5	0.26	0.65	1548.7	0.87	-	-	-	-	-
	10.5	0.33	0.48	1196.3	0.89	-	-	-	-	-
	11.5	0.30	0.56	1282.0	0.89	-	-	-	-	-
	12.5	0.23	0.45	1417.5	0.85	-	-	-	-	-
	13.5	0.30	0.40	1068.2	0.89	-	-	-	-	-
	14.5	0.07	0.52	1716.5	0.77	-	-	-	-	-
	15.5	0.33	0.24	1437.5	0.85	-	-	-	-	-
	16.5	0.32	0.38	-	-	-	-	-	-	-
	17.5	0.26	0.22	1700.1	0.79	-26.4	-22.7	-	54.1	50.3
	18.5	0.29	0.23	1782.9	0.80	-26.8	-23.1	-	54.5	50.7
	19.5	0.35	0.22	1303.7	0.86	-26.7	-23.9	-	54.4	51.5
	20.5	0.27	0.19	1660.0	0.80	-26.4	-	-	54.1	-
	21.5	0.31	0.13	1489.0	0.82	-26.6	-22.6	-	54.2	50.2
22.5	0.35	0.22	2230.8	0.78	-28.7	-23.1	-	56.4	50.8	
23.5	0.27	0.19	2076.9	0.76	-26.7	-22.9	-	54.3	50.6	
24.5	0.23	0.18	2227.8	0.72	-29.3	-21.2	-	56.9	48.9	
25.5	0.25	0.11	2472.4	0.69	-28.0	-22.6	-	55.7	50.2	
Core 3	1	0.24	0.09	1462.4	0.78	-25.3	-19.2	-18.7	53.0	46.9
	3	0.29	0.08	1338.7	0.81	-24.4	-20.8	-19.3	52.1	48.4
	5	0.22	0.10	1350.4	0.78	-24.8	-20.6	-	52.4	48.3

Core	Depth (cm)	AVS-S (wt. %)	Pyrite-S (wt. %)	Fe <sub>HCl</sub> (ppm)	DOS	$\delta^{34}\text{S}_{\text{AVS}}$ (‰)	$\delta^{34}\text{S}_{\text{Pyrite}}$ (‰)	$\delta^{34}\text{S}_{\text{organic}}$ (‰)	$\Delta^{34}\text{S}_{\text{SO}_4\text{-AVS}}$ <sup>*</sup> (‰)	$\Delta^{34}\text{S}_{\text{SO}_4\text{-Pyrite}}$ <sup>*</sup> (‰)
	7	0.18	0.13	779.5	0.85	-26.2	-21.2	-	53.9	48.9
	9	0.20	0.10	1236.8	0.78	-27.3	-21.7	-	55.0	49.3
<i>Oxic core</i>										
Core 9	1	0.06	0.04	910.8	0.62	-26.3	-	-16.5	48.8	-
	3	0.08	0.05	1086.3	0.62	-29.6	-	-16.9	52.1	-
	5	0.19	0.06	3085.7	0.56	-29.6	-	-	52.1	-
	7	0.15	0.06	3427.0	0.48	-29.5	-	-	52.0	-
	9	0.08	0.06	4878.7	0.28	-30.4	-	-	52.9	-
	11	0.06	0.03	1205.7	0.52	-31.4	-	-	54.0	-
	13	0.10	-	635.5	-	-32.0	-	-	54.5	-
	15	0.03	0.02	504.5	0.59	-33.3	-	-	55.8	-
	17	0.05	0.02	224.7	0.81	-33.5	-	-	56.0	-
	19	0.07	0.03	398.5	0.78	-32.5	-	-	55.0	-
	21	0.10	0.04	376.6	0.85	-32.0	-	-	54.5	-
	23	0.18	0.04	329.7	0.91	-34.8	-	-	57.3	-
	25	0.11	0.03	289.3	0.89	-33.6	-	-	56.1	-
	27	0.26	0.05	1070.0	0.82	-33.7	-	-	56.2	-
	29	0.25	0.05	682.0	0.88	-34.8	-	-	57.3	-

\* $\Delta^{34}\text{S}_{\text{SO}_4\text{-sulfide}}$  (where sulfide is either AVS or Pyrite) for Cores 2 and 3 are referenced to the average  $\delta^{34}\text{S}$  of pore water sulfate below the chemocline ( $\Delta^{34}\text{S} = 27.6\text{‰} - \delta^{34}\text{S}_{\text{sulfide}}$ ) and the isotopic offset for Core 9 is relative to pore water sulfate above the chemocline ( $\Delta^{34}\text{S} = 22.5\text{‰} - \delta^{34}\text{S}_{\text{sulfide}}$ ).

1 Table 3. Concentration and isotope data for pore waters extracted from Mahoney Lake sediment  
 2 cores recovered below the chemocline (Anoxic cores) and above the interface (Oxic core).

Core	Depth (cm)	SO <sub>4</sub> (mM)	Cl (mM)	ΣH <sub>2</sub> S (mM)	δ <sup>18</sup> O <sub>SO4</sub> (‰)	δ <sup>34</sup> S <sub>SO4</sub> (‰)	δ <sup>34</sup> S <sub>H2S</sub> (‰)	Δ <sup>34</sup> S <sub>SO4-H2S</sub> (‰)
<i>Anoxic cores</i>								
Core 2	3	409.8	63.9	11.68	18.1	27.4	-18.7	46.2
	5.5	505.3	67.2	12.51	19.3	26.6	-21.5	48.1
	6.5	418.5	64.0	20.68	18.8	27.4	-22.4	49.7
	7.5	427.5	66.5	20.29	19.2	27.2	-23.6	50.8
	9.5	428.0	66.4	17.40	-	28.5	-20.5	-
	15.5	447.4	69.3	4.67	-	28.4	-	-
	19.5	-	-	6.05	-	-	-	-
	26.5	-	-	0.56	-	-	-	-
Core 3	0.5	468.0	69.4	18.03	19.9	28.2	-21.0	49.2
	1.5	454.0	69.7	21.36	-	-	-	-
	2.5	431.4	71.7	17.71	-	-	-	-
	5.5	453.5	70.0	15.44	-	-	-	-
	6.5	422.3	69.8	28.15	20.4	27.9	-22.6	50.5
	7.5	445.8	69.4	3.80	19.6	28.1	-20.6	48.6
	8.5	-	-	-	18.4	27.6	-25.1	52.7
	9.5	457.5	69.2	21.38	21.3	28.5	-25.0	53.5
	15	466.7	66.9	7.03	-	-	-	-
	21	473.0	69.8	15.83	-	-	-	-
	41	459.1	64.2	15.48	-	-	-	-
	53	481.7	66.7	15.80	-	-	-	-
	59	430.6	68.1	18.66	-	-	-	-
	73	440.5	68.2	8.41	-	-	-	-
	83	510.7	68.2	20.86	-	-	-	-
<i>Oxic core</i>								
Core 9	1	321.1	55.5	1.44	17.8	22.2	-17.8	40.1
	3	301.5	50.9	1.85	-	22.6	-30.0	52.7
	5	300.6	48.7	2.14	17.3	22.6	-24.6	47.3
	7	305.5	49.5	0.62	-	23.1	-28.3	51.5
	9	292.8	47.3	1.95	17.5	22.4	-25.4	47.8
	11	306.5	46.7	1.93	-	22.5	-25.2	47.7
	13	300.3	50.3	1.31	17.6	22.5	-27.0	49.5
	15	299.9	51.1	1.87	-	22.6	-29.9	52.5
	17	296.3	52.3	1.85	17.9	22.5	-28.7	51.2
	19	297.1	50.5	1.80	-	22.6	-29.0	51.6
	21	296.3	53.0	1.75	17.4	22.4	-36.0	58.4
	23	303.4	52.2	1.70	-	22.4	-33.6	55.9
	25	295.0	52.6	1.38	17.7	22.7	-34.5	57.2
	27	293.5	52.6	1.90	-	22.5	-	-
29	290.3	57.3	1.38	-	22.3	-30.2	52.5	